DISSERTATIONES
GEOGRAPHICAE
UNIVERSITATIS
TARTUENSIS
66

LIISI JAKOBSON

Mutual effects of wind speed, air temperature and sea ice concentration in the Arctic and their teleconnections with climate variability in the eastern Baltic Sea region

DISSERTATIONES GEOGRAPHICAE UNIVERSITATIS TARTUENSIS
66

DISSERTATIONES GEOGRAPHICAE UNIVERSITATIS TARTUENSIS
66

LIISI JAKOBSON

Mutual effects of wind speed, air temperature and sea ice concentration in the Arctic and their teleconnections with climate variability in the eastern Baltic Sea region

UNIVERSITY OF TARTU
Press

Department of Geography, Institute of Ecology and Earth Sciences, Faculty of Science and Technology, University of Tartu, Estonia

Dissertation was accepted for the commencement of the degree of *Doctor philosophiae* in physical geography at the University of Tartu on 9 April 2018 by the Scientific Council of the Institute of Ecology and Earth Sciences, University of Tartu.

Supervisors: Professor Jaak Jaagus
Department of Geography, Institute of Ecology and Earth Sciences, University of Tartu, Estonia

PhD Erko Jakobson
Tartu Observatory, University of Tartu, Estonia

Opponent: Professor Joanna Wibig
Department of Meteorology and Climatology, University of Łódź, Poland

Commencement: J. G. Granö auditorium (room 327), Vanemuise 46, Tartu, on 19 June 2018 at 10.15 a.m.

Publication of this thesis is granted by the Institute of Ecology and Earth Sciences, University of Tartu

ISSN 1406-1295
ISBN 978-9949-77-730-3 (print)
ISBN 978-9949-77-731-0 (pdf)

University of Tartu Press
www.tyk.ee

CONTENTS

LIST OF ORIGINAL PUBLICATIONS

I Jakobson, E., Vihma, T., Palo, T., **Jakobson, L.,** Keernik, H., Jaagus, J.: Validation of atmospheric reanalyses over the central Arctic Ocean. *Geophysical Research Letters*, 39, 1–6, doi: 10.1029/2012GL051591, 2012.

II **Jakobson, L.,** Vihma, T., Jakobson, E., Palo, T., Männik, A., Jaagus, J.: Low-level jet characteristics over the Arctic Ocean in spring and summer. *Atmospheric Chemistry and Physics*, 13, 11089–11099, doi: 10.5194/acp-13-11089-2013, 2013.

III **Jakobson, L.,** Vihma, T., Jakobson, E., Jaagus, J. Relationships between sea ice concentration and wind speed in the Arctic during 1979–2015, Manuscript will be submitted for publication to the *Journal of Geophysical Research.*

IV **Jakobson, L.,** Jakobson, E., Post, P., Jaagus, J.: Atmospheric teleconnections between the Arctic and the eastern Baltic Sea regions. *Earth Systems Dynamics*, 8, 1019–1030, https://doi.org/10.5194/esd-8-1019-2017, 2017.

Author's contribution

I The author participated in wind speed theme in interpretation of results and preparation of the manuscript.

II The author is responsible for the study design, data processing and analysis except technical calculations using GrADS, interpretation of results, preparation of the manuscript and communicating with the Editorial Board.

III The author is the initiator of the study, responsible for the study design, data processing and analysis except technical calculations using GrADS, interpretation of results, preparation of the manuscript.

IV The author is responsible for original idea, study design, data processing and analysis except technical calculations using GrADS, interpretation of results, preparation of the manuscript and communicating with the Editorial Board.

LIST OF ABBREVIATIONS

AA	Arctic amplification
ABL	Atmospheric boundary layer
DAMOCLES	Developing Arctic Modelling and Observation Capabilities for Long-Term Environmental Studies
DJF	December, January, February
ECMWF	European Centre for Medium-Range Weather Forecasts
IPCC	Intergovernmental Panel on Climate Change
JJA	June, July, August
LLJ	Low-level jet, a low-altitude maximum in the vertical profile of the wind speed
MAM	March, April, May
METEX	Meteorological Data Explorer
NASA	National Aeronautics and Space Administration
NCEP-CFSR	National Centres for Environmental Prediction Climate Forecast System Reanalysis
NSIDC	National Snow and Ice Data Centre
RMSE	Root mean square error
S10	10 m wind speed
SBL	Stable boundary layer
SIC	Sea ice concentration
SLP	Sea level pressure
SON	September, October, November
TP	Testing point
WSR	Wind speed ratio between 10 m and 850 hPa level

ABSTRACT

In this thesis the key area of global climate change, the Arctic region, is investigated. Low-level jets (LLJ) are detected, wind vertical profile is studied, and near-surface wind interactions with sea ice are analysed. Also validation of reanalyses products are carried through in the central Arctic Ocean. Further, teleconnections between the Arctic region and the eastern Baltic Sea region are studied.

The present study is mostly based on the meteorological observations and reanalyses data. We used tethersonde sounding data from the drifting ice station Tara. The sounding period lasted from 25 April to 31 August 2007 and the measurements were carried out in the central Arctic Ocean. Results showed lower occurrence on LLJs than it was previously recorded from most of other studies. Probably due to the stable boundary layer (SBL), low-level jets that had baroclinic forcing mechanism, occurred at lower altitudes than other jets (which is not the case in other regions). Generation mechanisms of LLJs were detected as follows: 30% baroclinity, 9% non-baroclinic inertial oscillations, and 9% related to wind gusts. Whereas 40% of LLJs were associated with observed frontal passages and in these cases the causal reason for the jet generation was probably baroclinicity, inertial oscillations or gusts.

There are quite few observational data from central Arctic and these are commonly assimilated to reanalyses. We had a rare possibility to validate reanalyses with independent (not assimilated into models) in situ data. Wind speed, air temperature and air humidity were the parameters validated. The following reanalyses were included in the study: the European ERA-Interim, the Japanese JCDAS, and the U.S. NCEP-CFSR, NCEP-DOE, and NASA-MERRA. The first ranked was ERA-Interim, still, no single product seems to agree better in all fields with reference datasets. Although ERA-Interim outperformed the other reanalyses in the bias and root mean square error (RMSE) for air temperature as well as in the bias and RMSE for the wind speed; near-surface parameters as 10 m wind speed and 2 m air temperature were best captured by NCEP-CFSR.

NCEP-CFSR was used to investigate the Arctic key element, sea ice, and near-surface wind speed interaction. The prevailing negative correlations between sea ice concentration (SIC) and 10 m wind speed (S10) may originate from various dynamic and thermodynamic reasons, which may compensate each other and decrease the strength of correlations. The correlation that arises from inter-annual variability is much stronger than correlation from seasonal and synoptic variability. The effect of SIC to the vertical profile of wind speed was studied through correlations between SIC and wind speed ratio (WSR). The larger role of physical mechanism related to atmospheric stratification can be seen as the distinguished difference between summer and other seasons. In the central Arctic in summer the ice surface can be warmer than the open sea surface. During other seasons, where the temperature above ice is clearly colder

than above water, positive correlations between ice concentration and Richardson number (*Ri*) demonstrate that the decreasing sea ice generates less stable stratification. Less stable stratification allows more vertical mixing of momentum and, therefore, stronger near-surface winds.

The teleconnections between meteorological parameters of the Arctic and the eastern Baltic Sea regions were analysed based on the NCEP-CFSR reanalysis data for 1979–2015. The Baltic Sea region was characterised by meteorological values at a testing point (TP) in southern Estonia (58°N, 26°E). Temperature at the 1000 hPa level at the TP have a strong negative correlation with temperature in the Greenland sector (the region between 55–80°N and 20–80°W) during all seasons except summer. Significant teleconnections are present in temperature profiles from 1000 to 500 hPa. After using partial correlation for removal of the AO index variability, correlations in winter were below ±0.5, while in other seasons there remained regions with strong ($|R|>0.5$, $p<0.002$) correlations. The positive temperature anomaly of mild winter at the Greenland sector shifts towards east during the next seasons, reaching to Scandinavia/Baltic Sea region in summer. The most permanent lagged correlations in 1000 hPa temperature reveals that the temperature in summer at the TP is strongly predestined by temperature in the Greenland sector in the previous spring and winter.

1. INTRODUCTION

The global mean surface temperature has increased since the late 19th century. Each of the past three decades has been warmer at the Earth's surface than all the previous decades in the instrumental record (IPCC, 2013). At the same time, over the past half century, the Arctic region has warmed at about twice the global rate (IPCC, 2013; Walsh, 2014; Navarro et al., 2016). This disparity reached a new record level during 2016 (Sun et al., 2018). While the Arctic covers only a small fraction of the Earth, it plays a disproportionate and multi-faceted role in the climate system (Francis et al., 2017). The effect of accelerated warming in the Arctic region in comparison with that for the entire globe has been named the Arctic amplification (AA). However, the reasons behind the AA are not entirely clear (Serreze and Barry, 2011; Navarro et al., 2016).

One of the biggest problems in the investigations in the Arctic region is the spatial irregularity of data. The Arctic region provides challenging environments for data assimilation. Meteorological stations, which are difficult and expensive to establish and maintain, are sparsely distributed around the Arctic Ocean (Inoue et al., 2009; Sato and Inoue, 2018). The scatter between various climate model projections for the 21^{st} century is particularly large in the Arctic (Christensen et al., 2007; Takhsha et al., 2017). Climate models have large problems in simulating the recent changes in the Arctic sea ice cover (Stroeve et al., 2007; Rampal et al., 2011; Proshutinsky et al., 2016). Even the atmospheric reanalyses include major errors over the Arctic sea ice (Chaudhuri et al., 2014, Lindsay et al., 2014; Liu et al., 2015).

Atmospheric reanalyses are widely applied in the Arctic research. Reanalyses products have been improved all the time and new products have been developed. By the year 2012, when our validation of reanalyses was made, many new reanalyses products were developed (e.g. ECMWF ERA-Interim, JCDAS, NCEP CFSR, MERRA). In general, these new reanalyses applied better horizontal and vertical resolution, better sea-ice and land-surface schemes, more extensive assimilation of satellite data, and more sophisticated assimilation methods than the older products. Although several recent studies had evaluated these new reanalyses in the Arctic (Lüpkes et al., 2010; Screen and Simmonds, 2011; Cullather and Bosilovich, 2011; Cuzzone and Vavrus, 2011; Wilson et al., 2011), there was a strong need for a study applying independent in situ data for the validation. We had a rare opportunity to use unique data collected during the Tara expedition, which were not included into data assimilations and had a good vertical resolution. The Tara expedition was a part of the European Union Sixth Framework Programme project DAMOCLES (Vihma et al., 2008).

Errors in both climate models and numerical weather prediction models tend to be largest in the conditions of a stable boundary layer (SBL) (Tjernström et al., 2005; Atlaskin and Vihma, 2012; Walesby and Beare, 2016). There are several reasons that make SBL a challenge for atmospheric models (Steeneveld et al., 2006; Atlaskin and Vihma, 2012). One of them is related to low-level jets

(LLJ, a low-altitude maximum in the vertical profile of the wind speed), which commonly occur in conditions of a SBL. In a SBL, turbulence near the surface is weak. Hence, the wind shear below the core of a LLJ may be the main source of turbulence (Mahrt, 2002; Mäkiranta et al., 2011). This results in a top-down structure of the SBL. Further, a LLJ often occurs intermittently, so that the shear-driven turbulence is also intermittent, which is another major challenge for modellers (Costa et al., 2011; Mahrt, 2014). There are, however, not many detailed studies on the occurrence and generation mechanisms of LLJs over the Arctic sea ice. Insufficiency of high-resolution data on the vertical profiles of wind speed is the largest impediment for exploring LLJs over the Arctic Ocean. Based on the high vertical resolution data from the Tara expedition we had the opportunity to carry through the first recording of the characteristics and generation mechanisms of LLJs in the central Arctic Ocean. Some mechanisms that elsewhere generate jets (e.g. terrain effects and the diurnal cycle) are not active over a flat sea ice surface very close to the North Pole. Better knowledge of LLJs in data sparse areas, such as the Arctic, gives the opportunity to improve the physical model of different climate and numerical weather prediction models and atmospheric reanalyses.

Arctic sea ice is a key element of the Arctic climate system. The importance of investigations of polar sea ice as a crucial element of Arctic ecosystem has been broadly emphasised (Deser and Teng, 2008; Comiso et al., 2008; Budikova, 2009; Ogi and Rigor, 2013; Stroeve et al., 2014; Vihma, 2014; Gao et al., 2015; Koenigk et al., 2016). The negative trend of sea ice extent which has been present at least since the mid-20th century has accelerated in recent years (Walsh and Chapman, 2001; Stroeve et al., 2007; Stroeve et al., 2012; Brown and Arrigo, 2012; Simmonds, 2015; Connolly et al., 2017). The sea ice melt season has become longer (Maksimovich and Vihma, 2012) and sea ice has become thinner (Chevallier et al., 2017). Its drift velocities have increased (Stroeve et al., 2012), and sea ice extent has decreased in every season, and in every decade since 1979 (IPCC, 2013). Different meteorological parameters and phenomena have complex relationships with sea ice in the Arctic. Besides the increase of temperature, changes in oceanic circulation, cloud cover, and amount of water vapour, the changes of atmospheric circulation and especially near-surface winds have their important role in the shrinking of sea ice (Watanabe and Ogi, 2013). The positive ice-temperature feedback is broadly known and investigated (Serreze and Francis, 2006; Screen and Simmonds, 2010). We had a hypothesis that there is also a two-way interaction between sea ice and near-surface wind. The dynamic impact of winds on the Arctic sea ice has been discussed extensively (Proshutinsky and Johnson, 1997; Hutchings et al., 2005; Ogi et al., 2010; Graversen et al., 2011; Herman and Glowacki, 2012; Watanabe and Ogi, 2013). It is probable that also the shrinking sea ice cover increases near-surface wind speed. Decreasing sea ice concentration should yield increasing near-surface wind speed because of less stable stratification and lower surface roughness. This two-way interaction between ice concentration and near-surface winds may amplify the changes.

Unprecedented warming in the Arctic and its possible feedbacks open up different climatological and ecological circumstances and may influence other regions of the World. These Arctic influences could be direct, as the advection of cold and dry air from over the ice-covered areas to the neighbouring territories, but it could also be through teleconnections – the large-scale patterns of high- and low-pressure systems and circulation anomalies that cover vast geographical areas and reflect the non-periodic oscillations of the climate system. Teleconnections between the Arctic and mid-latitude regions have been the focus of research for many years and several reviews about the Arctic sea ice impact on the global climate (Budikova, 2009; Vihma, 2014) or Eurasian climate (Gao et al., 2015) have been published. Several studies have demonstrated relationships between warming and/or ice decline, and mid-latitude weather and climate extremes (Petoukhov and Semenov, 2010; Francis and Vavrus, 2012; Tang et al., 2013; Petoukhov et al., 2013; Coumou et al., 2014; Handorf et al., 2015). Other studies have analysed whether these associations are statistically and/or physically robust (Barnes, 2013; Screen and Simmonds, 2013, 2014; Hassanzadeh et al., 2014; Screen et al., 2014; Barnes et al., 2014). Some investigations suggest that the apparent associations may have their origin, in part, in remote influences (Screen et al., 2012; Sato et al., 2014; Peings and Magnusdottir, 2014; Perlwitz et al., 2015). According to Overland et al. (2015) potential Arctic teleconnections with Europe are less clear than with North America and Asia. As far as we know, there have been no previous studies on the topic, how the Arctic region may influence on climate variability in the eastern Baltic Sea region. Although some parameters, especially air temperature and humidity have quite high spatial correlation between surrounding regions, still the eastern Baltic Sea region is a distinct region with its vicinity to polar front. By tracking down the teleconnections between the rapidly changing Arctic region and the eastern Baltic Sea region we can get valuable information about possible future trends even if the changes in both regions were caused by a third factor.

The specific objectives of this thesis are as follows:

- to validate and choose the best reanalyses products for investigating different climatic parameters in the Arctic (I);
- to document and characterise low-level jets (LLJ) in the central Arctic (II);
- to analyse interactive relationships between sea ice and near-surface winds (III);
- to find possible links in climate variability between different Arctic regions and the eastern Baltic Sea region (IV).

2. DATA

2.1. Observational meteorological data

Meteorological observations from the drifting ice station Tara were carried out in the central Arctic Ocean from March to September 2007 (Figure 1). The tethersonde sounding period lasted from 25 April to 31 August (Vihma et al., 2008).

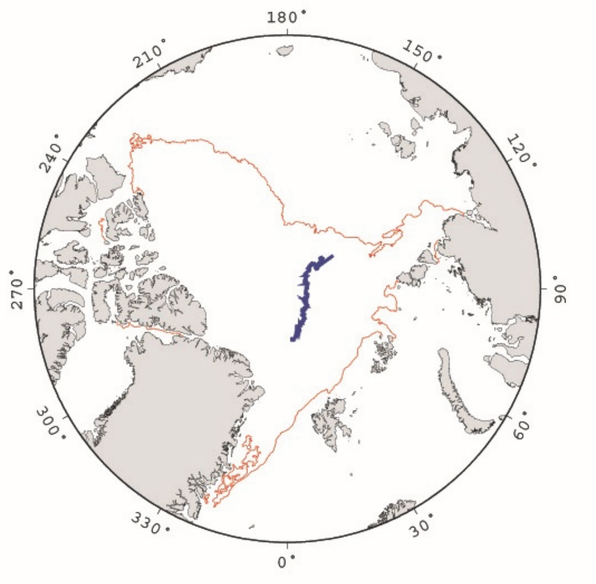

Figure 1. Drift trajectory of Tara (blue) from the period of tethersonde soundings: 25 April to 31 August, 2007. The brown line shows the September minimum sea ice extent.

A Vaisala DigiCORA Tethersonde System was used to measure the vertical profiles of the wind speed, air temperature, relative humidity, and wind direction (Vihma et al., 2008). The tethersonde system consisted of a 7 m^3 balloon filled by helium, tetherline, winch, and three sondes with 20 m vertical intervals. Due to the risk of breaking the balloon or tetherline, the measurements were only carried out under wind speeds lower than 15 m s^{-1} in the whole profile. The balloon was ascended as high as possible (the average top height of the soundings was 1240 m), and the data were recorded with about 5 m intervals. Though the winch was spooling with constant speed of 1 to 1.5 m s^{-1}, the balloon did not gain height with a constant speed. The balloon did not rise up straight but drifted along the wind. The recorded wind speed values were systematically higher during descent than ascent (usually from 0.5 to 2 m s^{-1}). Hence, an average profile was calculated (for each sensor separately) on the basis of the ascending and descending profiles. This averaging (over every 20 m) yields more reliable results, although some information on temporal variations is lost. In addition to tethersonde soundings, the air temperature and wind speed were measured at a 10 m high weather mast (Aanderaa AWS 2700) at the heights of 1, 2, 5 and 10 m, the air relative humidity and air pressure at 2 m and wind direction at 10 m.

2.2. Reanalyses

Reanalysis is a systematic approach to produce multidecadal, gridded datasets that estimate a large variety of atmospheric, sea-state, and land surface parameters, including many that are not directly observed (Dee et al., 2014a). Reanalyses are created via an unchanging ("frozen") data assimilation scheme and model(s), which ingest all available observations every 6–12 hours over the period being analysed. This unchanging framework provides a dynamically consistent estimate of the climate state at each time step. One component which still does vary in reanalyse models is the sources of the raw input data. This is unavoidable due to the ever changing observational network which includes, but is not limited to, radiosonde, satellite, buoy, aircraft and ship reports. Currently, approximately 7–9 million observations are ingested at each time step. Over the duration of each reanalysis product, the changing observation mix can produce artificial variability and spurious trends (Dee et al., 2014b). Still, such datasets have become fundamental to research and education in the earth sciences (Dee et al., 2014a). In data sparse areas, such as the Arctic, reanalyses are the best available source of integrated information on the four-dimensional structure of the atmosphere (Screen and Simmonds, 2011). Extensive work has recently been carried out to improve reanalyses. In the Arctic region three reanalyses stand out as being more consistent with independent observations: NCEP-CFSR, MERRA, and ERA-Interim (Lindsay et al., 2014). Still, Chaudhuri et al. (2014) summarized that no single product seems to agree better in all fields with reference datasets. Monthly seasonal means (DJF, MAM, JJA, SON) were calculated from the 6-hourly data. Monthly mean wind speed was calculated as a scalar average not as magnitude of wind speed monthly means u- and v-components vectorial sum.

ERA-Interim is a global atmospheric reanalysis produced by the European Centre for Medium-Range Weather Forecasts (ECMWF). Data are available with resolution approximately 80 km on 60 vertical levels. According to Lindsay et al. (2014) ERA-Interim is one of the three models that stand out as being more consistent with independent observations. However, comparisons against observations show that in the Arctic ERA-Interim have near-surface positive biases in temperature and humidity (Liu et al., 2015).

JCDAS is a global atmospheric reanalysis produced by the Japan Meteorological Agency (JMA), which is continuation of JRA-25 (Onogi et al., 2007). Data are available with a horizontal grid spacing of around 120 km and 40 vertical layers. With the relatively simplified treatment of ice concentration in JCDAS (based on a 55% concentration threshold), the temperature is significantly underestimated in the quasi-ice-covered area and overestimated in ice-free area (Inoue et al., 2011). Unexpected erroneous open sea along the coast of the Arctic Ocean was found for the years from 1979 to 1981 and from 1991 to 1993 (Onogi et al., 2007).

MERRA (Modern Era-Retrospective Analysis for Research and Applications) is a global atmospheric reanalysis produced by NASA (National Aeronautics and Space Administration) (Rienecker et al., 2011). Data are available with resolution 65 km on 72 vertical levels. MERRA is one of the three models that stand out as being more consistent with independent observations in Arctic (Lindsay et al., 2014). However, Serreze et al. (2012) report that the MERRA record shows evidence of artefacts in the lower tropospheric temperature and humidity in the region north of 70°N.

NCEP-CFSR (Climate Forecast System Reanalysis) and NCEP-DOE (Department of Energy) are global atmospheric reanalyses produced by The National Centres for Environmental Prediction (NCEP). The CFSR global atmosphere resolution is ~38 km with vertical 64 levels (Saha et al., 2010); whereas DOE resolution is 210 km with 28 vertical levels. For the period 1979–2010, data of CFSR version 1 (Saha et al., 2010) were used; for 2011–2015, CFSR version 2 were used.

2.3. NSIDC ice concentration

The National Snow and Ice Data Centre (NSIDC) specializes in remote sensing of snow and ice, Arctic climate, frozen ground, ice sheets, glaciers, and more. From 1978, the sea ice concentration passive microwave data are available. From NSIDC database, Bootstrap Sea Ice Concentrations from Nimbus-7 SMMR and DMSP SSM/I-SSMIS, Version 2 (Cavalieri et al., 1996) were used (version 0051, horizontal resolution is 1°, temporal resolution is two days).

2.4. METEX air backward trajectories

The Meteorological Data Explorer (METEX), developed at the Centre for Global Environmental Research (CGER), includes programs for calculating air trajectory and for visualizing meteorological fields. The site (http://db.cger.nies.go.jp/metex/trajectory.html) provides service for online trajectory calculations, which utilizes the NCEP/NCAR reanalysis, trajectory length from 72 to 240 hours. We used 72 h backward trajectories to investigate origin of the LLJs. The air mass origin was divided into five sectors (Figure 8 in Publication II): (1) 20°W–30°E (the Fram Strait region), (2) 30–165°E (the Russian Arctic), (3) 165–210°E (the region towards the Bering Strait), (4) 210–340°E (the western Arctic), and (5) the vicinity of the North Pole (northward of 85°N).

3. METHODS

3.1. Models validation

All reanalyses products were horizontally linearly interpolated to Tara sounding sites. In the vertical, the reanalysis results were linearly interpolated from the reanalysis output levels to the sounding levels. In addition, the diagnostic reanalysis products for 2 m temperature and humidity and 10 m wind speed were validated. For all variables, the bias, root mean square error (RMSE) and correlation coefficient against observations were calculated, as well as the statistical significance of the bias and correlation in 95% confidence level. Correlation coefficients between observed and modelled air temperature and specific humidity were high, often exceeding 0.9, but these were due to the strong seasonal change from spring to summer, which was naturally captured by the reanalyses. Hence, for temperature and specific humidity, we only report correlations calculated using the 19 summer soundings. We define summer as the period with the Tara 2 m air temperature above –1 ºC: from 9 June to 31 August (Vihma et al., 2008). The temperature inversion base height, depth, and strength was defined as in Kahl (1990) using a threshold of 0.3 ºC for the temperature increase with height (Vihma et al., 2011). A layer with a specific humidity increase larger than 0.2 g kg^{-1} was considered as a humidity inversion.

3.2. LLJ definitions and causal mechanisms

A LLJ was defined following Stull (1988) as the level with a local wind speed maximum of more than 2 m s^{-1} greater than wind speeds above it. Jet variables are defined on Figure 2. The level of maximum wind was defined as the jet core (z_j). The difference between z_j and the subsequent wind speed minimum above (z_a) was defined as the jet depth ($z_a - z_j$). The wind speed difference between the core speed (U_j) and the minimum speed above (U_a) were defined as the jet strength ($U_j - U_a$). The level of maximum air temperature was defined as the temperature inversion top (z_t). The difference between the z_t and the previous temperature minimum below (z_b) was defined as the temperature inversion depth ($z_t - z_b$). The air temperature difference between the inversion top temperature (T_t) and the minimum temperature below (T_b) was defined as the temperature inversion strength ($T_t - T_b$). In the illustrated example sounding from 10 August 2007, the data allow identifying a LLJ in the wind speed profile with a core speed of 8.4 m s^{-1} at the height of 180 m. The wind is remarkably weak near the surface and around 800 m. The top of inversion (230 m) is slightly above the jet core (180 m). The inversion strength is only 1.6 ºC, but the jet strength (5.7 m s^{-1}) is larger than the average observed at Tara.

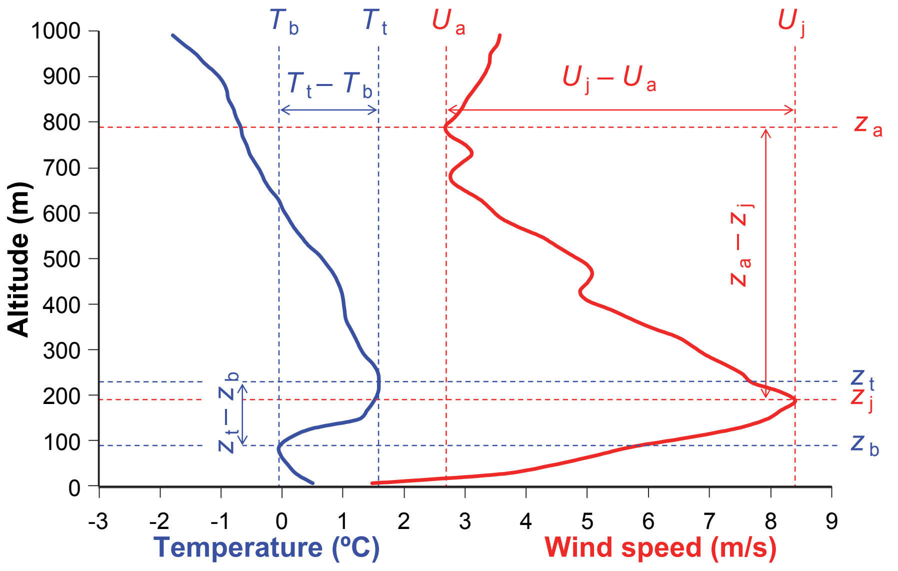

Figure 2. Example of a tethersonde sounding at 13 UTC on 10 August 2007. The variables plotted are wind speed and temperature, provided as an illustration of the definitions used.

In the sounding period from 25 April to 31 August, there were a total of 95 soundings in 39 sounding days. For LLJ statistics, one sounding per day was selected. Such a selection was needed because the LLJs observed were not necessarily independent of each other (up to eight soundings per day were made). To count the occurrence of LLJs, the highest sounding per day was chosen. To count the other properties of LLJs, the existence of a LLJ was the criteria for choosing the daily sounding (one or more LLJs were observed in 25 of the 39 days). From sounding days with more than one LLJ observed, the highest sounding with a LLJ was chosen. All the observed LLJ profiles were used in analyses of the generation mechanisms of LLJs (43 profiles among 95 soundings). To summarize, we had a total of 95 soundings, LLJs observed in 43 of these, and 25 soundings were included in analyses of LLJ properties.

Static stability was defined as the bulk-Richardson number (*Ri*), which is a non-dimensional parameter describing the ratio of buoyancy and wind shear in turbulence production (e.g. Kaimal and Finnigan, 1994). As Andreas et al. (2000), we calculated *Ri* from the surface to each observation height:

$$Ri(z) = \frac{gz}{\Theta(z)} \frac{\Theta(z) - \Theta_s}{v^2(z)} . \tag{1}$$

Here, g is the acceleration of gravity; z is the observation height; $\Theta(z)$ and $v(z)$ are the potential temperature and wind speed at z; and Θ_s is the potential temperature at the height of 10 m, which was the first averaging height of the tethersonde data (in cases of LLJs, the 10 m temperature was within ± 0.3 °C of the 1 m temperature recorded in the weather mast). If $Ri(z)$ was smaller than the critical Richardson number (Ri_{cr}), the layer up to the height z was considered to be turbulent. The Ri_{cr} has no unambiguous value; empirically based suggestions in the literature range from 0.2 to 1.0 (Galperin et al., 2007). We took $Ri_{cr} = 0.4$, similarly to Andreas et al. (2000). The lowest level for which $Ri(z) \geq Ri_{cr}$ is indicated as z_{Ri} and is assumed to be the top of the turbulent layer.

Baroclinity related to the horizontal temperature gradient may generate a LLJ at the level above which the decreasing geostrophic wind dominates and below which the effect of surface friction dominates. Air temperature fields based on the ECMWF operational analyses were used to identify the cases with geostrophic wind speed decreasing with height.

The equations for thermal wind are as follows (e.g. Stull, 2009):

$$\frac{\partial U_g}{\partial z} = -\frac{g}{f_c T}\frac{\partial T}{\partial y}, \quad (2)$$

$$\frac{\partial V_g}{\partial z} = +\frac{g}{f_c T}\frac{\partial T}{\partial x}. \quad (3)$$

Here, U_g is the eastward and V_g the northward component of geostrophic wind; f_c is the Coriolis parameter; T is the temperature; x and y are coordinates towards east and north, respectively. The geostrophic wind speeds at the surface and at z_a were calculated. If the geostrophic wind speed was at least 2 m/s smaller at z_a than at surface, the baroclinity criteria was fulfilled.

Inertial oscillations related to the Coriolis force and ceasing of frictional drag may induce a LLJ later at night (Blackadar, 1957) or after storms, when the stable stratification is re-established (Andreas et al., 2000). LLJs generated by inertial oscillations typically have their core close to the top of the stable boundary layer (Thorpe and Guymer, 1977; Andreas et al., 2000). As it is not possible to give exact criteria for the threshold stratification for occurrence of turbulence, potentially inertial jets we classified. These were jets that have their core above the lowest level where $Ri \geq 0.2$ but below the lowest level where $Ri \geq 0.7$.

Wind gusts are typically generated by downward turbulent transport of momentum from higher altitudes (Suomi et al., 2012). Hence, in a tethersonde-based individual wind profile, a wind speed maximum at some layer may be simply due to a wind gust. This was studied by comparing the ascending and descending profiles (their time difference at the jet core height was never larger than 1 h). If a jet is only present in one of them, it suggests the influence of a gust.

Front wasn't considered to be a causal generation mechanism for LLJs, but a front is a favourable environment for LLJ generation. This is because (a) non-occluded fronts are baroclinic, (b) in case of a cold front, the cold air mass typically penetrates below the warm air mass, building a stably stratified layer in between, which favours the generation of inertial oscillations, and (c) wind in the cold air mass is very often gusty (Wallace and Hobbs, 2006). To detect fronts, the tethersonde soundings, surface-layer meteorological observations and the ECMWF operational analyses were utilized.

3.3. Sea ice and near-surface wind speed

To control the accuracy of NCEP-CFSR ice concentration the comparison with NSIDC (National Snow and Ice Data Centre) (Cavalieri et al., 1996) passive microwave measured ice concentration was carried through. Comparison showed that the difference of averages of ice concentration in percentage is smallest in central Arctic (where the correlation between ice concentration of two models is weakest) and largest in ice edge region (up to 8%). At ice edge region the correlation between NCEP-CFSR and NSIDC is mostly more than 95%. Hence, we presume that NCEP-CFSR ice concentration data is sufficiently accurate.

Richardson number is calculated similarly to LLJ methods (eq. 1).

In this work, we used two different correlation coefficients – inter-annual and synoptic scale. Inter-annual correlations are calculated on the basis of seasonal means. Synoptic-scale correlations are firstly calculated on the bases of 6-hourly data separately for each season and for each year and averaged thereafter seasonally.

3.4. Teleconnection analyses

The eastern Baltic Sea region was characterised by meteorological values at a testing point (TP) in southern Estonia (58°N, 26°E). We defined the Greenland sector as region between 55–80°N and 20–80°W. The correlation coefficient for the seasonal mean air temperature at 1000 hPa between the TP and different sub-basins of the eastern Baltic Sea is mostly higher than 0.85, the same for SLP. The highest correlation is observed in winter and the lowest in summer.

Linear correlation coefficients were calculated to reveal teleconnections between the Arctic region and the TP of the eastern Baltic Sea region. Only linear Pearson correlations were used, non-linear correlations were not included. For correlations with the TP, the first correlation input was taken at the TP and the second in the Arctic region.

To remove from the correlations the effect of atmospheric teleconnections which could be described by known teleconnection indices, partial correlations between selected meteorological parameters with the controlling effect of the teleconnection indices were calculated.

Cold and mild winters were defined as years when the winter average temperature differed the whole period average more than one standard deviation at a geographical point in the Greenland sector (70°N, 60°W). Accordingly – cold winters were 1983, 1984, 1989, 1990, 1992 and 1993; mild winters were 1980, 1985, 1986, 2003, 2007, 2009, 2010 and 2011.

For revealing the possible delayed dependences between the atmospheric variables of the Arctic region and the TP, lagged analysis was carried through. For the lagged correlation, there has to be time shift between the two data series. We have organized it so that the second parameter was taken by lag months earlier than the first parameter.

4. RESULTS

4.1. Validation of atmospheric reanalyses over the central Arctic Ocean

Atmospheric reanalyses (ERA-Interim, JCDAS, NCEP-CFSR, NCEP-DOE, and MERRA) were validated against independent in situ data (see more Section 2.1) on air temperature, air humidity and wind speed.

The mean profile of air temperature over the 29 soundings wasn't captured by any of the reanalyses (Figure 3a). ERA-Interim and MERRA performed very well above 200 m, but had a significant warm bias of up to 2.0 ºC at lower levels. NCEP-CFSR was very good in the lowermost 200 m layer, but had a significant cold bias above 400 m. Results from JCDAS strongly deviates from observations. Considering RMSE (Figure 3b), ERA-Interim outperformed the other reanalyses ranging from 1.9 to 3.0 ºC. NCEP-CFSR had a clearly smallest RMSE close to the surface. Most of the temperature errors larger than 7.5 ºC (20 cases of 23) occurred when the wind speed averaged over the profile was higher than 6 m/s. Besides, all three exceptions were from the JCDAS model. From the 29 measured profiles, 23 included a temperature inversion and 21 had a humidity inversion.

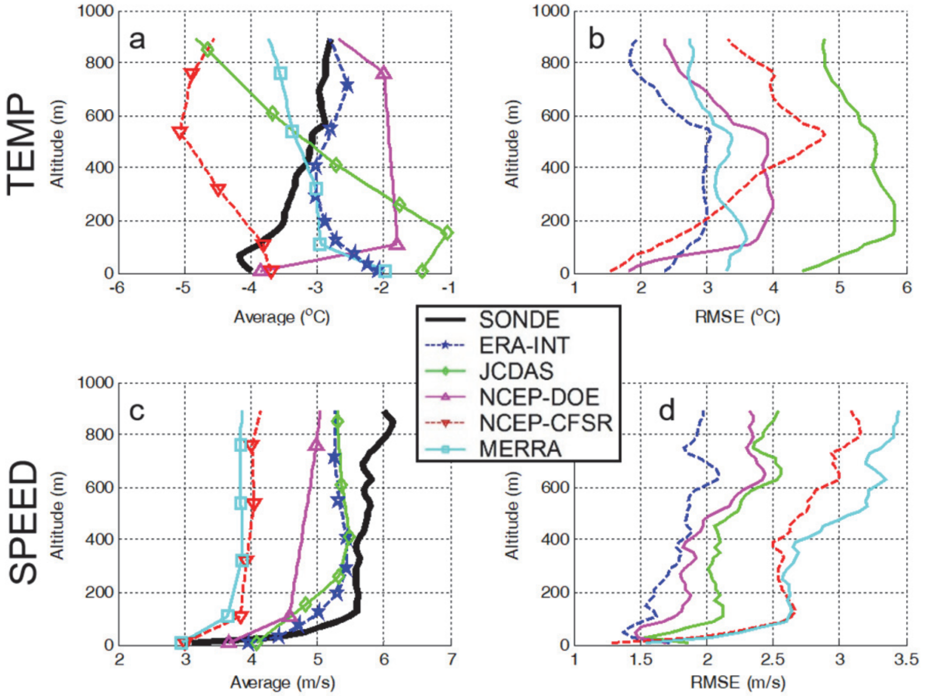

Figure 3. From 29 single profiles calculated: (a) average temperature, (b) RMSE (root mean square error) of temperature, (c) average wind speed, (d) RMSE of wind speed.

The best reanalysis capturing both temperature and humidity inversions was NCEP-DOE (only 4 missing and 2 false temperature inversions; 6 missing and 4 false humidity inversions) and the worst JCDAS (11 missing and 1 false temperature inversions; 17 missing and 3 false humidity inversions).

The mean wind speed profile (over the 29 soundings) was best captured by ERA-Interim and JCDAS with the magnitude of the negative bias smaller than 0.6 m s^{-1} (Figure 3c). At all model levels, NCEP-DOE underestimated wind speed by 1 m s^{-1} and NCEP-CFSR and MERRA by 1.7–1.8 m s^{-1} (Figure 3c). NCEP-CFSR and MERRA, however, outperformed the other reanalyses for the 10 m wind speed. The RMSE for the 10 m wind speed was approximately 1.5 m s^{-1} for all reanalyses (Figure 3d). At higher levels ERA-Interim was clearly the best, followed by NCEP-DOE and JCDAS, while the new NCEP-CFSR and MERRA reanalyses were clearly the worst.

Table 1. Vertically averaged values of the magnitude of bias, RMSE, and correlation coefficient of air temperature (*Ta*), specific humidity (*Qa*), relative humidity (*RH*), and wind speed (*V*).

	ERA-Interim		**NCEP-DOE**		**NCEP-CFSR**		**MERRA**		**JCDAS**	
	Mean	**Rank**	**Mean**	**Rank**	**Mean**	**Rank**	**Mean**	**Rank**	**Mean**	**Rank**
***Ta* |bias|**	0.51	**5**	1.17	**3**	1.36	**2**	0.63	**4**	1.42	**1**
***Ta* RMSE**	2.61	**5**	3.31	**3**	3.53	**2**	3.15	**4**	5.30	**1**
***Ta* Correl**	0.74	**4**	0.79	**5**	0.70	**2**	0.74	**3**	0.63	**1**
***Qa* |bias|**	0.40	**1**	0.20	**4**	0.14	**5**	0.33	**2**	0.25	**3**
***Qa* RMSE**	0.75	**4**	0.81	**2**	0.54	**5**	0.75	**3**	0.81	**1**
***Qa* Correl**	0.56	**4**	–0.17	**1**	0.58	**5**	0.33	**2**	0.47	**3**
***RH* |bias|**	6.89	**2**	2.35	**5**	5.82	**3**	5.26	**4**	8.68	**1**
***RH* RMSE**	15.7	**3**	15.9	**2**	15.3	**5**	15.4	**4**	16.8	**1**
***RH* Correl**	0.41	**3**	0.48	**4**	0.29	**2**	0.52	**5**	0.23	**1**
***V* |bias|**	0.43	**5**	0.90	**3**	1.69	**2**	1.85	**1**	0.47	**4**
***V* RMSE**	1.80	**5**	2.03	**4**	2.70	**2**	2.91	**1**	2.20	**3**
***V* Correl**	0.71	**5**	0.59	**4**	0.44	**2**	0.28	**1**	0.52	**3**
Total points		**46**		**40**		**37**		**34**		**23**

To summarize the results we present a ranking of the reanalyses, with the bias, RMSE and correlation of air temperature, specific and relative humidity, and wind speed, vertically averaged over the 890 m layer (Table 1). ERA-Interim was ranked first; it outperformed the other reanalyses in the bias and RMSE for air temperature as well as in the bias, RMSE, and correlation coefficient for the wind speed (Table 1). The NCEP-CFSR, NCEP-DOE, and NASA-MERRA reanalyses outperformed the other reanalyses with respect to 2 m air temperature and specific humidity and 10 m wind speed, which makes them, especially NCEP-CSFR, better in near-surface research.

4.2. Low-level jets over the Arctic Ocean in spring and summer

4.2.1. Generation mechanisms of low-level jets

In spring and summer 2007 LLJs were analysed in the central Arctic Ocean. All the observed LLJ profiles from the drifting ice station Tara were applied in the analyses (43 profiles among 95 soundings; see more in Section 3.2) to investigate generation mechanisms. LLJs can be generated by a variety of mechanisms, including (a) baroclinity, (b) inertial oscillations (c) gusts, and (d) fronts.

Analyses showed that 30% of LLJ cases were detected as baroclinic jets and 7% of these cases were also detected as potentially generated by inertial oscillations (see below). For baroclinic jets, the mean jet strength ($U_j - U_a$) was 0.9 m s^{-1} larger than for jets which had no baroclinity forcing mechanism (confidence level $p < 0.05$). The mean jet core height (z_j) of baroclinic jets (265 m) occurred 172 m lower than in the case of other jets ($p < 0.01$). The baroclinity forcing mechanism was more important in July and August (85% of cases) than in April – June (15% of cases). From all LLJ cases, 16% were classified as potentially inertial oscillation jets (see more in paragraph 3.2). Note that LLJs generated by baroclinity can also have their core heights in the above-mentioned layer. In fact, 7% of cases were also detected as baroclinic ones. Jets that were potentially generated by inertial oscillation had 1.5 m s^{-1} higher ($p < 0.05$) wind speed at jet core (U_j) than jets which had no inertial oscillation forcing mechanism. The wind gust as generation mechanism was detected in about 9% of cases.

In about 12% of all LLJ cases, the 6-hourly ECMWF analyses showed a front within a distance of about 800 km of Tara. All these LLJ cases were classified above as generated by (a) baroclinity, (b) inertial oscillations or (c) gusts. In addition to the fronts detectable from the ECMWF analyses, during days with a LLJ observed, seven weaker frontal passages were observed at Tara, seen as rapid changes in the wind, air temperature, air humidity and radiative fluxes. As many as 40% of LLJs were observed during these frontal passages but not classified as generated by baroclinity, inertial oscillations or gusts. Probably, in each case, one or more of these mechanisms contributed to the generation of the

LLJ. The high number of such frontal LLJs is partly due to the fact that four frontal passages were observed in four days with frequent soundings. Only about 12% of the 43 cases the generation mechanism remained entirely unclear, but in these cases the jet strength was weak, only from 2.1 to 3.1 ms^{-1}.

4.2.2. Properties of low-level jets

The Tara results showed a lower occurrence of LLJs (46%) than many previous studies over polar sea ice. To count the occurrence of LLJs, the highest sounding per each day was chosen. To count the properties of LLJs, 25 cases were included (see Section 3.2; Publication II). The jet core typically occurred at a height of 100–500 m, but the lowest one was measured at 70 m and highest at 1150 m height. On average, baroclinic jets were located lower and jets generated by gust higher than the others. The most common depth of jet was 400 to 600 m; only two sounding profiles showed a jet depth exceeding 1 km. There were more baroclinic jets among jets that had a larger depth. The average jet core wind speed (U_j) was 7.1 m s^{-1} (note that measurements were carried out only during winds lower than 15 m s^{-1}). Most of jets of unknown forcing mechanisms had a larger wind speed than average but a weaker jet. Jets with the highest absolute wind speed were not the strongest ones. If all soundings had reached the height of 2 km, there might have been some more cases of a stronger and deeper jet.

Sounding data showed that a jet core with higher than average wind speed ($U_j > 7.1$ m s^{-1}) occurred more often inside the turbulent layer (77% of these cases showed $z_j < z_{Ri}$). Jet cores with smaller than average wind speed ($U_j < 7.1$ m s^{-1}) appeared above the turbulent layer (83% of these cases showed $z_j > z_{Ri}$). The jet core height (z_j) and the height of the top of temperature inversion z_t correlated ($r = 0.62$; $p < 0.01$; Figure 4). If the LLJs were inside the turbulent layer, there was no significant correlation between z_j and z_t. LLJs with the core above the turbulent layer had this coefficient of 0.72 ($p < 0.01$).

The 72-h backward trajectory calculations (Section 2.4) showed that in most cases the air mass including a LLJ originated from the sea ice zone, with only 28% of cases from the open ocean. Even during these cases, the air mass had travelled 800–1300 km over sea ice, as Tara was close to the North Pole. Soundings with LLJ cases had twice more western Arctic air masses and almost twice less Russian Arctic air masses than soundings without LLJ. All LLJs originating from the Fram Strait region (see more Section 3.2) were located inside the turbulent layer ($z_j < z_{Ri}$) whereas all LLJs originating from the Russian Arctic (20%) were located above the turbulent layer ($z_j > z_{Ri}$). In all cases of the Fram Strait sector (16%), the air mass had been over the open sea less than 72 h before the LLJ was observed at Tara. The LLJ cases originated from the vicinity of the North Pole (24%) showed some differences from the other LLJs. The average jet depth of these cases was as much as 356 m larger ($p < 0.05$) than in the case of other jets, and the mean z_a was 631 m higher ($p < 0.01$) than in the case of other LLJs.

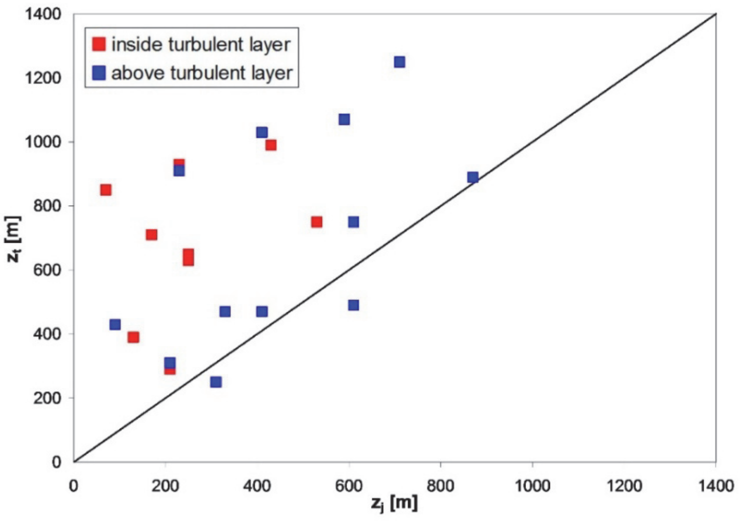

Figure 4. A comparison of the height of the jet core, z_j, with the height of temperature inversion top, z_t. LLJs are divided into two groups with the core inside or outside the turbulent layer.

4.3. Interactions between sea ice concentration and wind speed

At first, the trends of 10 m wind speed (S10) and sea ice concentration (SIC) were investigated to analyse interactions between them further. Prevailing negative trend of SIC is present in the Arctic Ocean. Most prominent season is autumn and most prominent regions are coastal regions, especially the Chukchi Sea and the Barents Sea (both up to –20% per decade). Results from other scientists support our findings (Table 1 in the Publication III). The trend of S10 is mainly positive, also most prominent in coastal regions, especially in the Chukchi Sea and the Barents Sea (both up to 10% per decade; Table 2 in the Publication III). The trend on wind speed ratio (WSR) is prevailingly positive. Trends highly depend on the season.

Different time scales were used to better understand the causal reasons for the correlations between SIC and S10. The correlation coefficient of inter-annual variations was strongly negative over most of the Arctic. The correlations that arise from inter-annual variability were much stronger than correlations that arise from synoptic variability. The standard deviation of S10 is larger in synoptic scale (annual average 1–2 m/s) than in inter-annual scale (annual average 0.5–1 m/s). SIC synoptic standard deviation annual average is 0.01–0.02, in inter-annual scale the SIC standard deviation annual average in the central Arctic Ocean is 0.05, in coastal regions it is much higher.

The strong winds may cause opening of leads and polynyas in some locations and packing of ice in another locations (see more in Discussion). To investigate which processes and where are dominating, the number of SIC increasing minus decreasing days after wind higher than 5 m/s were analysed. During autumn there are many regions with positive correlations in coastal areas, it means the packing effect is present there. Overall, most of time the SIC is decreasing after strong winds (Figure 5 in Publication III).

The effect of SIC to the vertical profile of wind speed was studied through correlations between SIC and wind speed ratio (WSR). In comparison of correlations between SIC and S10, there is evident large-scale positive correlation between SIC and WSR in the Arctic Ocean in summer (Figure 5). The distinguished difference between summer and other seasons show the larger role of physical mechanism related to ABL stratification (see more in Discussion).

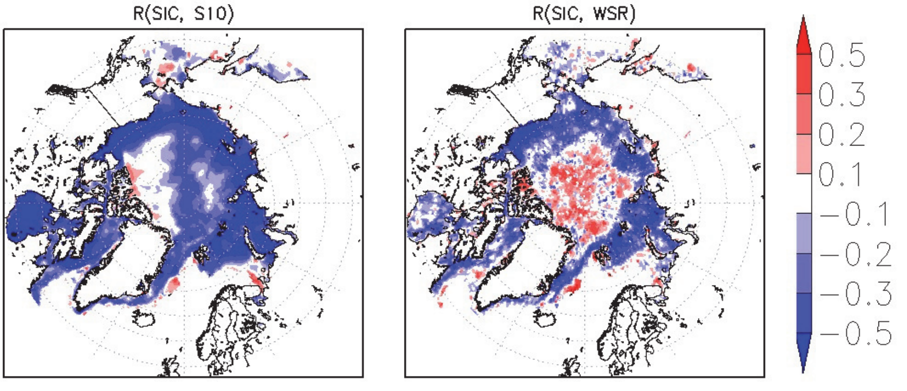

Figure 5. Inter-annual correlation coefficients between SIC and S10 (left) and between SIC and wind speed ratio (WSR) (right) in summer during 1979–2015.

As in the case of correlations between SIC and S10, also here the correlations between SIC and WSR are much higher for inter-annual than synoptic variability. The variations in the WSR are large but variations in ice concentration are much smaller.

In winter, the negative correlations between SIC and WSR in inter-annual time scales are particularly strong in the Barents, Kara and Laptev seas, i.e. in the marginal seas where inter-annual variations in the SIC are larger than in areas closer to the Canada Basin. In winters with small (large) SIC, the WSR is large (small), which follows to effect of ABL stratification. During summers, the interaction in the central Arctic is opposite. Summers with lots of ice in the central Arctic have high WSR. The larger role of physical mechanism related to ABL stratification can be also seen as the distinguished difference between summer and other seasons in correlation between SIC and *Ri* at 950 hPa. Positive correlation during other seasons have replaced with mainly insignificant correlation and some regions with negative correlation in summer (Figure 6).

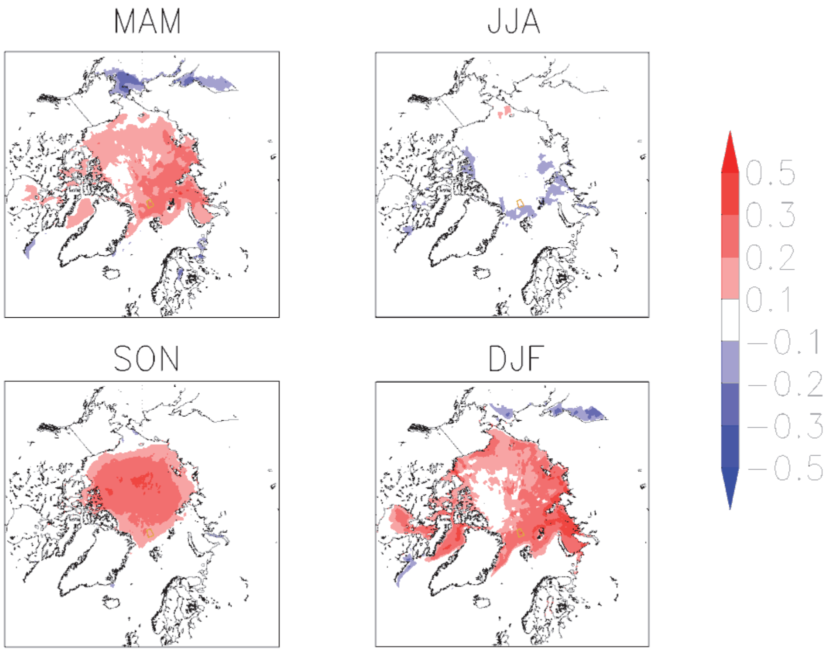

Figure 6. Correlation coefficients between the SIC and Richardson number (*Ri*) at 950 hPa for different seasons during 1979–2015.

4.4. Atmospheric teleconnections between the Arctic and the eastern Baltic Sea regions

4.4.1. Spatial correlations of climatic variables

Correlations of climatic variables at separate grid points depend highly on the distance and on climatic variables. For example, the spatial correlation remains significant for much longer distances than for precipitation as the processes of their formation are different. Besides the short distance correlation of climatic parameters between the testing point (TP) in southern Estonia (58°N, 26°E) and the surrounding grid points, there are also vast areas far from it still having significant correlations. The Greenland sector showed most often significant correlations with the parameters of the eastern Baltic Sea region. In Table 1 there are given spatial average, minimum and maximum values of seasonal correlations between the TP and the Greenland sector. Strong negative correlation in the Greenland sector at 1000hPa temperature in winter and spring decreases with altitude and turns even positive at 250hPa (Table 1). Specific humidity at 1000 hPa shows quite similar values with temperature at the same level. The correlation between wind speed at 1000hPa at the TP and the Greenland sector is mostly negative in winter, reaching up to −0.72. The most significant correlation between SLP is present in autumn and summer (Table 1).

Table 1. Areal average, minimum and maximum of seasonal correlations between VAR1 at TP and VAR2 at the Greenland sector (20–80°W, 55–80°N).

			AVER AGE			**MINIM UM**			**MAXI MUM**				
VAR1	**VAR2**	**DJF**	**MAM**	**JJA**	**SON**	**DJF**	**MAM**	**JJA**	**SON**	**DJF**	**MAM**	**JJA**	**SON**
t1000	**t1000**	–0.41	–0.23	0.15	–0.02	–0.63	–0.51	–0.22	–0.49	0.03	0.21	0.44	0.49
t850	**t850**	–0.41	–0.26	0.09	–0.02	–0.63	–0.46	–0.19	–0.34	0.08	0.06	0.34	0.48
t500	**t500**	–0.32	–0.19	0.24	0.00	–0.52	–0.51	0.02	–0.20	0.09	0.15	0.49	0.40
t250	**t250**	0.31	0.20	–0.02	0.00	0.08	0.02	–0.36	–0.29	0.55	0.39	0.41	0.28
q1000	**q1000**	–0.44	–0.20	0.28	–0.04	–0.65	–0.50	–0.19	–0.53	0.11	0.09	0.62	0.45
s1000	**s1000**	–0.11	0.02	0.05	0.01	–0.72	–0.58	–0.47	–0.36	0.77	0.67	0.75	0.42
SLP	**SLP**	0.15	–0.12	–0.25	–0.36	–0.25	–0.30	–0.43	–0.54	0.51	0.33	0.16	–0.13
t1000	**SLP**	–0.39	–0.27	–0.23	0.03	–0.73	–0.50	–0.42	–0.45	0.35	0.11	–0.02	0.51
t1000	**s1000**	–0.15	–0.03	–0.02	–0.03	–0.67	–0.54	–0.42	–0.65	0.65	0.48	0.38	0.43
t1000	**icec**	0.17	0.11	–0.07	0.01	–0.26	–0.34	–0.62	–0.41	0.61	0.64	0.41	0.48
s1000	**icec**	0.19	0.06	0.03	0.16	–0.28	–0.67	–0.36	–0.24	0.63	0.63	0.71	0.59

Climatic variables have close relationships between themselves. If there is a climatic change in one parameter, for example in temperature, then it causes changes also in other parameters connected with it, for example in ice concentration. Similarly to correlations of the same climate variable at the TP and the Arctic, there are significant correlations (|R|>0.5) between different climate variables at the TP and the Greenland sector. The temperature and wind speed at the 1000 hPa in the TP have significant teleconnection with the sea ice concentration in some regions of the Arctic Ocean in all seasons (Figure 7).

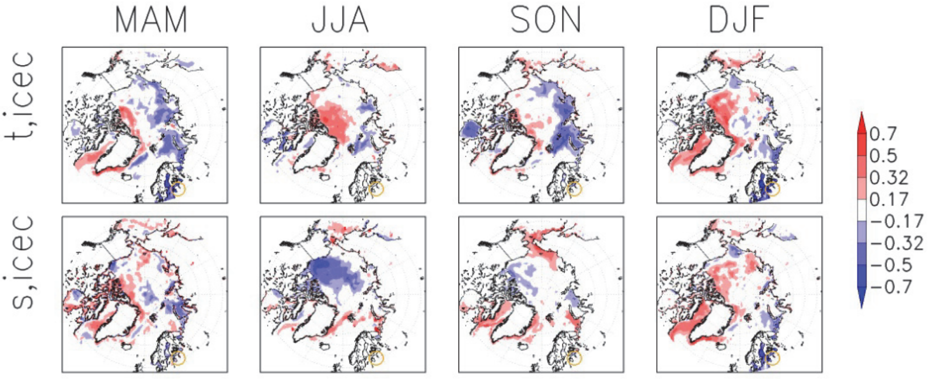

Figure 7. Correlation maps between seasonal mean values measured in the TP (the yellow circle) and in the whole Arctic region. Row 1: temperature on the 1000 hPa level in the TP and sea ice concentration; row 2: wind speed on the 1000 hPa level in the TP and sea ice concentration. Columns represent seasons, shading levels ±0.17 and ±0.32 represent correlation significance at the confidence levels 68% and 95%.

To reveal the impact of teleconnection indices to above-mentioned correlations between the TP and the Arctic region, partial correlations were carried through. The strongest impact had AO and NAO indices. Partial correlations with the controlling factor AO index reduce the area with a statistically significant correlation around the TP in all parameters and in all seasons. In winter the effects of the AO indices on spatial correlations are the strongest, up to 0.5. In spring, the differences between partial correlations with the AO indices are below 0.2 in the whole region compared to the regular correlations between the TP and the Arctic. In summer and autumn, the differences are even smaller than in spring. Partial correlation in temperature, after removing the influence of the AO index, is below ±0.5 on all levels (1000, 850, 500 and 250 hPa) in winter, though the regular correlations are the strongest (Table 2 in Publication IV). In other seasons, regions with stronger partial correlations than ±0.5 remain. Considering the correlation coefficients between seasonal mean temperatures, specific humidity, wind speed at the 1000 hPa level and SLP at the TP the AO indices have mostly higher correlations than the NAO indices, only SLP in summer and autumn has a significantly higher correlation with the NAO index.

The climate system consists of various interactive components that have highly various response times. The estimated timescales in the atmosphere grow with height and reach up to months, but due to atmospheric interactions with the oceans and cryosphere, the conditions in the atmosphere may have even longer response times. For finding the effect of the previous seasons on atmospheric conditions at the TP, lagged correlations were calculated for the 1000hPa temperature (Figure 8). The previous winter season has a strong effect on temperature during the following spring (lag=3) and summer (lag=6). At the same time, the winter mean temperature has almost no dependence on weather conditions during the previous seasons. There is a strong ($R > 0.5$) positive correlation between the 1000hPa temperatures at the TP in spring and in Eurasia during the previous winter (lag=3).The spring temperature is determined by the temperature of neither the previous autumn (lag=6) nor the previous summer (lag=9). Summer temperature at the TP has a strong positive correlation in the Greenland sector with the previous spring (lag=3), winter (lag=6), and autumn (lag=9). Autumn temperature at the TP has a strong negative correlation with the Fram Strait in the previous summer (lag=3) and the Taimyr region in the previous winter (lag=9) (Figure 8).

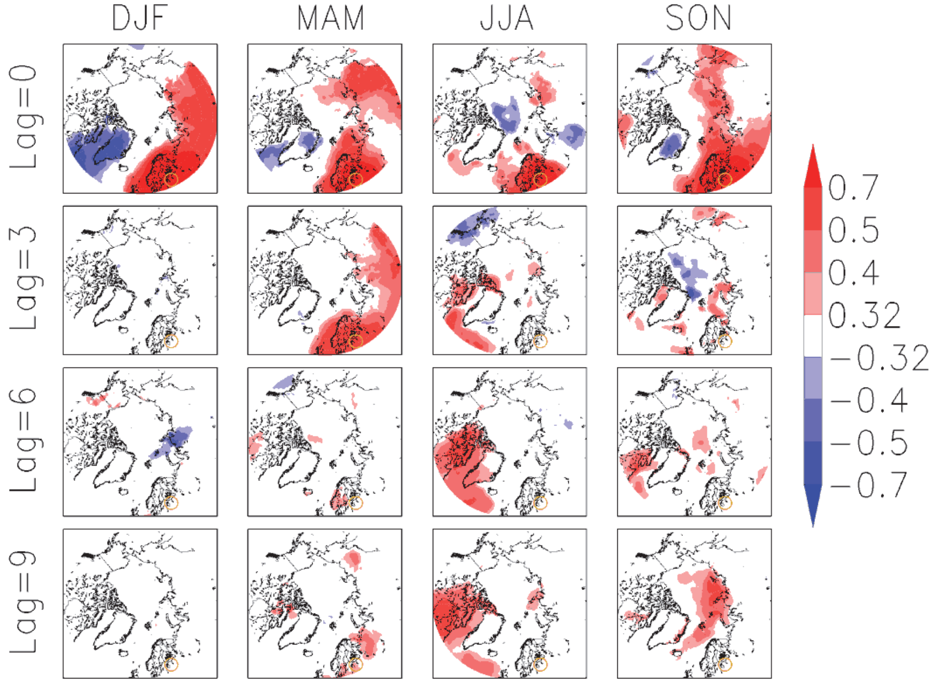

Figure 8. Lagged correlation maps between the TP (the yellow circle) and Arctic 1000hPa temperature: row 1, lag is 0 months (no lag); row 2, lag is 3 months; row 3, lag is 6 months; row 4, lag is 9 months. Columns represent seasons; all presented correlations are significant at the confidence level 95%.

4.4.2. Possible mechanisms of teleconnection

To compare broad atmospheric circulation patterns, we turn to the difference map of the geopotential heights of 500 hPa and temperature at 1000 hPa by subtracting the composites of cold winters (DJF) from those of mild winters (Figure 9). The geopotential heights of 500 hPa are more than 100 gpm higher in mild winters than in cold ones. The maximum of this height anomaly is centred over the maximum of the 1000 hPa temperature difference. The whole column (up to 500 hPa) of the air in the Greenland sector is warmer than at cold years.

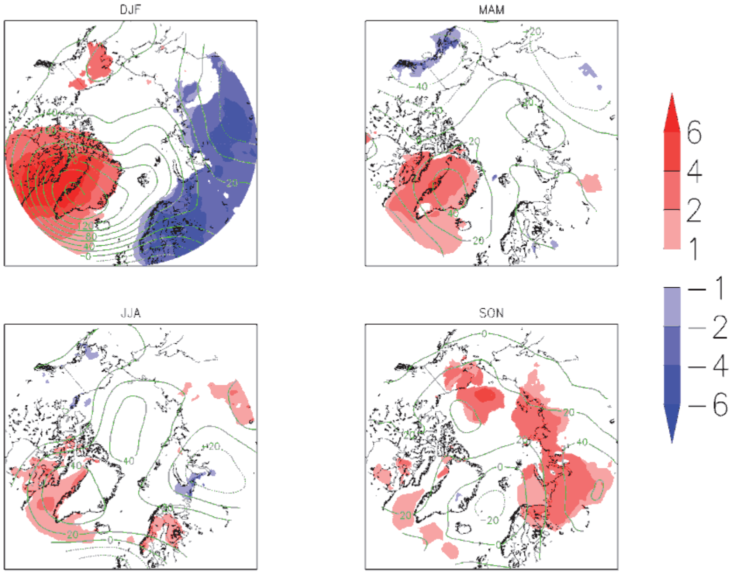

Figure 9. Seasonal difference maps (years with mild winters minus years with cold winters) in air temperature at 1000 hPa level (shading with confidence level of 95%), and geopotential height at 500hPa level (contours).

Ensuing summer shows positive values of the 1000 hPa temperature and the geopotential heights of 500 hPa in the Greenland sector and also Scandinavia region. The significant 1000 hPa temperature correlation between winter in the Greenland sector and ensuing summer in TP can be followed by lagged analyses. It shows a significant positive correlation between summer temperature at the TP and in the Greenland sector with the previous winter (Figure 6 in Publication IV). The annual evolution of 500 hPa height differences at 60°N shows that the positive height anomaly at the Greenland sector shifts towards east during the next seasons (Figure 5 in Publication IV). The propagation of the mid-tropospheric anomalies in this region is nonlinear: these height anomalies are significant only over some areas and months and in May they are slightly negative. Also at 65°N the similar pattern is present, but at 70°N and 75°N this kind of signal propagation is missing.

5. DISCUSSION

All validated reanalyses products showed large errors in the vertical profiles of air temperature and humidity, and NCEP-CFSR and MERRA also had large errors in the wind speed profile. Combining the validation results for temperature, humidity and wind, ERA-Interim got the highest overall ranking. ERA-Interim outperformed the other reanalyses in the bias and RMSE for air temperature as well as in the bias, RMSE, and correlation for the wind speed. Whereas, both NCEP reanalyses and MERRA outperformed the other reanalyses with the respect to 10 m wind speed, 2 m air temperature and specific humidity. This is an important result for those who apply reanalyses to provide atmospheric forcing for sea ice models in retrospective simulations. If one reanalysis should be selected for near-surface boundary layer, NCEP-CFSR is recommended on the basis of Publication I; it was among the best for all near-surface variables validated here. It should be remembered, however, that also radiative fluxes and precipitation, not validated in this study, are essential in the atmospheric forcing for sea ice. As the near-surface variables depend on a complex interaction of various processes, it is very difficult to evaluate what is the reason for the success of NCEP-CFSR. We only note that this reanalysis includes a comparably sophisticated treatment of sea ice, including its fractional coverage and prognostic ice and snow thickness (Saha et al., 2010).

The difficulties in improving reanalyses are demonstrated by the fact that the older NCEP-DOE outperformed the new NCEP-CFSR for the overall ranking. NCEP-DOE was the best reanalysis capturing both temperature and humidity inversions, though the model had the most sparse vertical resolution. JCDAS was the weakest model in capturing temperature and humidity inversions. The average temperature profile was close to moist-adiabatic, which suggests that the boundary layer scheme yields too much mixing. JCDAS results for the wind speed were, however, almost as good as those of ERA-Interim. An interesting aspect in the validation results was that the largest air temperature errors did not occur in conditions of very stable stratification, which is usually the case (Atlaskin and Vihma, 2012), but in conditions of higher-than average wind speeds. This may be related to the large role of lateral advection in controlling the air temperature variability over the Arctic Ocean, especially in spring and summer 2007 (Graversen et al., 2011). The observed biases in wind speed, temperature, and humidity are in many cases comparable or even larger than the climatological trends during the latest decades (Serreze et al., 2009). This calls for caution when applying reanalyses data in climatological studies. Still, while reanalyses are the best available source of integrated information on the four-dimensional structure of the atmosphere in the Arctic region, it is important to choose most appropriate model for specific research.

The Tara tethersonde soundings probably represent the best data set of LLJs over the central Arctic Ocean from April through August (although late summer has been better covered by ship-based observations (Tjernström et al., 2012)).

According to Publication II the Tara results showed a lower occurrence of LLJs (46±8%) compared to 60–80% of ReVelle and Nilsson (2008) over polar oceans and 80% of Andreas et al. (2000) over the Antarctic sea ice. According to our understanding, the most important reasons for the relatively low occurrence of LLJs at Tara were that (a) the observations were made far from strongly baroclinic zones, such as the sea ice margin, and (b) the typical conditions in April – August were not as stably stratified than in the autumn – winter data set of Andreas et al. (2000). Another data with a low occurrence of LLJs (25%) were the Arctic Ocean Expedition 2001 soundings, which were taken far from the ice edge (Tjernström et al., 2004). Outcome of Publication II showed that jets with a high U_j occurred mostly inside the turbulent layer, and jets with a low U_j above the turbulent layer. Strong jet core winds contribute to growth of the turbulent layer, i.e., there is a two-way interaction between the ABL structure and LLJs. Previous studies have indicated some correlation between the jet core height z_j and the temperature inversion top height z_t ($r = 0.53$ in a climatology of LLJs over the USA (Bonner, 1968)). Findings from Publication II revealed a more complex relationship: if the jet core was inside the turbulent layer, there was no significant correlation between z_j and z_t, whereas $r = 0.72$ ($p < 0.01$) was observed for cases with the jet core above the turbulent layer. This is probably related to the situation that in conditions of a strong temperature inversion, the turbulent layer is thin and inertial oscillations prevail, generating a jet close to z_t. Contrary to previous studies (Smedman et al., 2001); in the Tara data the baroclinic jets occurred at lower altitudes than other jets. This is probably due to the fact that the core height of a baroclinic LLJ is determined by the frictional retardation of the stronger geostrophic winds below, and the frictionally affected layer is shallow under stable stratification.

The prevailing negative correlations between SIC and S10 may originate from various dynamic and thermodynamic reasons, which may compensate each other and decrease the strength of correlations. The strong winds can cause opening of leads and polynyas (Figure 10c) in some locations and packing of ice (Figure 10b) in another locations. The net effect of strong winds is to decrease the ice concentration in all time scales from synoptic to inter-annual. Another factor is that strong winds in the Arctic are typically associated with advection of warm, moist air masses from lower latitudes (Figure 10d) (e.g. Vihma and Pirazzini, 2005), whereas weak winds are typical in high-pressure conditions. Advection from lower latitudes may generate stable stratification (e.g. Vihma et al., 2003) or bring weakly or neutrally stratified air to the Arctic (Figure 10e). A reduced sea ice concentration favours unstable stratification (Figure 10f) (Francis et al., 2009; Overland and Wang, 2010; Jaiser et al., 2012; Vihma, 2014), allowing more vertical mixing of momentum and, hence, stronger near-surface winds (Figure 10g) (Sweet et al., 1981; Wallace et al., 1989; Hayes et al., 1989; Takatama el al., 2015). Decreasing sea ice concentration also influences surface roughness (Figure 10h). For small SIC the decreasing SIC yields smaller surface roughness (i.e. positive correlation), but if sea SIC decreases from 100% to about like 70%, the aerodynamic roughness length increases (i.e. negative correlation), as there are more floe edges, which generate form drag (Lüpkes et al., 2013). The correlation between SIC and S10 (and WSR) is stronger and trends of these parameters are more prominent in the regions where SIC is less than 70% (coastal regions). So here, the shrinking sea ice decrease the surface roughness and increase the near-surface winds.

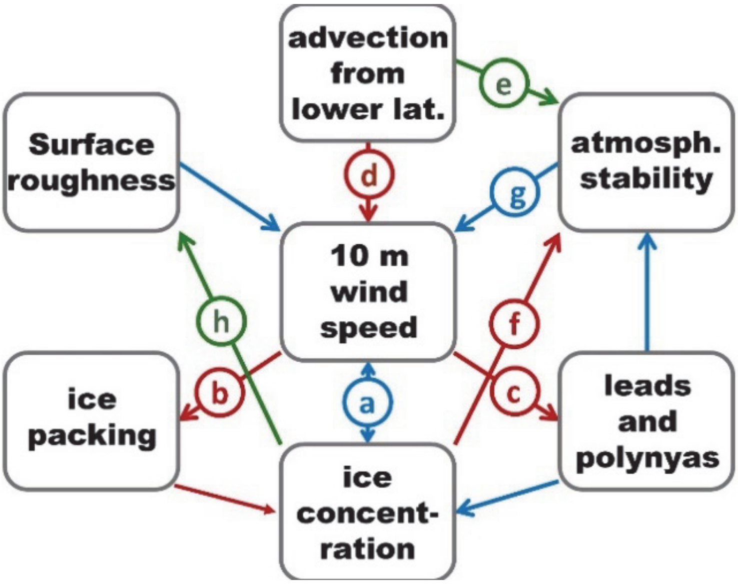

Figure 10. A schematic figure illustrating the two-way interactions between wind and sea ice concentration. Blue arrows present negative interactions, red arrow positive interactions and green arrows present interactions that are either negative or positive, depending on the conditions.

Stronger negative correlation when calculated on the basis of inter-annual instead of synoptic variability we interpret as follows. Considering different time scales the standard deviation of SIC and S10 is quite different. The impact of SIC on S10, both short- and long-term variations in SIC can either decrease or increase S10 via the surface roughness effect (Figure 10h), i.e. the dynamic effect is not systematic. A systematic thermodynamic effect of SIC on S10 is stronger, if the anomalies in ice concentration last longer (Figure 10f). Considering the impact of S10 on SIC, wind speed varies a lot without always affecting SIC, in particular in synoptic time scale. On the other hand, in inter-annual time scales, variations in S10 are related to different large-scale circulation regimes in the Arctic and have a strong thermodynamic impact on SIC. Hence, it is understandable that the inter-annual correlations are stronger than the synoptic ones. The reason of distinguished difference between summer and other seasons in SIC correlation with WSR and *Ri* 950 is connected to the reverse surface temperature contrast between water and sea ice. In the central Arctic in summer the ice surface is typically warmer than the open sea surface.

As since the melting snow and sea ice as well as the water in the melt ponds have temperatures very close to 0 °C, but the open ocean in leads has surface temperatures close to the freezing point of saline sea water. If the temperature above ice is warmer, Richardson number may grow (it means ABL is more stable*)* with shrinking ice. During other seasons, where the temperature above ice is clearly colder than above water, positive correlation between ice concentration and Richardson number demonstrate that the decreasing sea ice generates less stable stratification. Less stable stratification (smaller *Ri* number value) allows more vertical mixing of momentum and, therefore, stronger near-surface winds.

Teleconnections between the Arctic and the mid-latitude regions has been the focus of researches for many years already. As far as we know there have been no previous studies on the topic how the Arctic region may influence on climate variability in the eastern Baltic Sea region. According to Publication IV strong negative correlation between the eastern Baltic Sea region and Greenland sector in temperature at the 1000 hPa level is similar to the correlations with the AO and NAO index. It is probably partly induced by the general circulation of the atmosphere. These correlations can be considered as an effect of stronger westerlies that carry relatively warm and moist air from the North Atlantic into Eurasia and, at the same time, cold and dry air from the central Arctic to Greenland and the Canadian Arctic Archipelago.

Although some scientist have claimed that the NAO index may be physically more relevant and robust for the Northern Hemisphere variability than is the AO index (Ambaum et al., 2001; Bader et al., 2011, Uotila et al., 2015); others declare opposite results. Thompson and Wallace (1998) declared that the AO index is actually more strongly coupled to the Eurasian winter surface air temperature than the NAO index. Rinke et al. (2013) showed through the coupled regional climate model experiments that atmospheric large-scale circulation in a winter following a low September sea ice resemble a negative AO pattern. Our results show that for the correlation coefficients between the eastern Baltic Sea region and the Greenland sector, the AO index had mostly the highest impact in every season, only SLP in summer and autumn had a significantly stronger impact with the NAO index. The positive temperature anomaly at 1000 hPa height shifts from the Greenland sector in winter towards east. Our lagged analyses showed that the summer temperature at TP has significant correlation with Greenland sector in winter (JJA; lag=6).

6. CONCLUSIONS

In this thesis, valuable drifting ice station Tara observational data were used to characterise, for the first time low-level jets and their generation mechanisms in the central Arctic. The Tara observational data, which were not included to data assimilations, were used to validate most common reanalyses products used in the Arctic. Since reanalyses are widely applied in the Arctic research and many scientists have reported large errors, there is a strong need for validation with independent data. This obtains the knowledge of choosing the best product depending on parameters scientists are dealing with. The best reanalyses product for investigating near-surface variables turn out to be NCEP-CFSR. It was used to reveal interactions between 10 m wind speed and the key element of the Arctic climate system – the sea ice. The teleconnections between meteorological parameters of the Arctic and the eastern Baltic Sea regions were analysed to get knowledge for possible future trends of the eastern Baltic Sea region.

Main findings of this thesis can be concluded as follows:

- In contrary to most of the earlier LLJs research in the Arctic and in the Antarctic, according to drifting ice station Tara data, the occurrence of LLJs is much lower (46±8%) instead of 60–80%.
- Analyses showed that the most important clearly identified causal mechanism of LLJs was baroclinity (30%); also potentially inertial oscillation jets (16%) and the wind gust (9%) were detected. Almost half of the LLJs observed were associated with frontal passages.
- Differently from other LLJs studies from other regions our data showed that jets with baroclinic forcing mechanism occurred at lower altitudes than other jets. This is probably due to the fact that the core height of a baroclinic LLJ is determined by the frictional retardation of the stronger geostrophic winds below, and the frictionally affected layer is shallow under stable stratification.
- According to independent in situ validation in the central Arctic Ocean ERA-Interim got the highest overall ranking; it outperformed the other reanalyses in the bias and root mean square error (RMSE) for air temperature as well as in the bias, RMSE, and correlation coefficient for the wind speed.
- The NCEP-CFSR, NCEP-DOE, and MERRA reanalyses outperformed the other reanalyses with respect to 2 m air temperature, specific humidity and 10 m wind speed, which make them, especially NCEP-CSFR, the best choice for near-surface analyses.
- Based on data from NCEP-CFSR reanalysis clearly negative correlation between sea ice concentration and wind speed at 10 m in all time scales from synoptic to inter-annual exists. During winter, spring and autumn the decreasing sea ice generates less stable stratification, which leads to stronger near-surface winds.

- Strong teleconnections are present between different climate variables at the eastern Baltic Sea testing point and the Arctic. Temperature and wind speed at the 1000 hPa level in the eastern Baltic Sea region have in all seasons strong teleconnections with the sea ice concentration in some regions of the Arctic Ocean. These teleconnections cannot be explained solely with the climate indices variability.

Pathways for further research:

- The first step is done by recording LLJs with generation mechanisms in the central Arctic. It helps better to understand top-down structure of the stable boundary layer in the Arctic, which is important to modellers to improve both climate models and numerical weather prediction models. However, the whole Arctic is in a big change, and also LLJs should be recorded after a time interval.
- Our results showed that there is a two-way interaction between ice concentration and near-surface winds. Especially ice concentration but also near-surface winds are in changeable face right now. Further investigation is needed to predict this amplifying change which influences the whole Arctic climate system and also southward regions.
- Statistical relationships between parameters of the eastern Baltic Sea region and some Arctic regions were found. Further analyse is needed to reveal the physical causes of these interactions between these regions.

REFERENCES

Ambaum, M.P., Hoskins, B.J., Stephenson, D.B.: Arctic Oscillation or North Atlantic Oscillation? J CLIMATE, 14, 3495–3507, doi: http://dx.doi.org/10.1175/1520-0442(2001)014<3495:AOONAO>2.0.CO;2, 2001.

Andreas, E.L., Claffey, K.J., and Makshtas, A.P.: Low-level atmospheric jets and inversions over the Weddell Sea. BOUND-LAY METEOROL, 97, 459–486, doi: 10.1023/A:1002793831076, 2000.

Atlaskin, E., and Vihma, T.: Evaluation of NWP results for wintertime nocturnal boundary-layer temperatures over Europe and Finland. Q J ROY METEOR SOC, 138, 1440–1451, doi: 10.1002/qj.1885, 2012.

Bader, J., Mesquita, M.D.S., Hodges, K.I., Keenlyside, N., Østerhus, S., Miles, M.: A review on Northern Hemisphere sea-ice, storminess and the North Atlantic Oscillation: Observations and projected changes. ATMOS RES, 101, 809–834, doi: 10.1016/j.atmosres.2011.04.007, 2011.

Barnes, E.A.: Revisiting the evidence linking Arctic Amplification to extreme weather in midlatitudes. GEOPHYS RES LETT, 40, 4734–4739, doi: 10.1002.grl.50880, 2013.

Barnes, E.A., Etienne, D.S., Giacomo, M., and Woollings, T.: Exploring recent trends in Northern Hemisphere blocking. GEOPHYS RES LETT, 41, 638–644, doi: 10.1002/2013GL058745, 2014.

Blackadar, A.K.: Boundary layer wind maxima and their significance for the growth of nocturnal inversions. B AM METEOROL SOC, 38, 283–290, 1957.

Bonner, W.: Climatology of the low level jet. MON WEATHER REV, 96, 833–850, doi: 10.1175/1520-0493(1968)096<0833:COTLLJ>2.0.CO;2, 1968.

Brown, Z. W. and Arrigo, K. R.: Contrasting trends in sea ice and primary production in the Bering Sea and Arctic Ocean. ICES J MAR RES, 69, 1180–1193. doi: 10.1093/icesjms/fss113, 2012.

Budikova, D.: Role of Arctic sea ice in global atmospheric circulation: A review. GLOBAL PLANET CHANGE, 68, 149–163, doi: 10.1016/j.gloplacha.2009.04.001, 2009.

Cavalieri, D.J., Parkinson, C.L., Gloersen, P., and Zwally, H.J.: Sea ice concentrations from Nimbus-7 SMMR and DMSP SSM/I-SSMIS passive microwave data, version 1. [subset 0051]. Boulder, Colorado USA. NASA National Snow and Ice Data Centre Distributed Active Archive Centre. doi: https://doi.org/10.5067/8GQ8LZQVL0VL, 1996.

Chaudhuri, A.H., Ponte, R.M., and Nguyen, A.T.: A comparison of atmospheric reanalysis products for the Arctic Ocean and implications for uncertainties in air–sea fluxes. J CLIMATE, 27, 5411–5421, doi: http://dx.doi.org/10.1175/JCLI-D-13-00424.1, 2014.

Chevallier, M., Smith, G.C., Dupont, F., Lemieux, J.-F., Forget, G., Fujii, Y., Hernandez, F., Msadek, R., Peterson, K.A., Storto, A., Toyoda, T., Valdivieso, M., Vernieres, G., Zuo, H., Balmaseda, M., Chang, Y.-S., Ferry, N., Garric, G., Haines, K., Keeley, S., Kovach, R.M., Kuragano, T., Masina, S., Tang, Y., Tsujino, H., and Wang, X.: Intercomparison of the Arctic sea ice cover in global ocean–sea ice reanalyses from the ORA-IP project. CLIM DYNAM, 49, 1107–1136, https://doi.org/10.1007/s00382-016-2985-y, 2017.

Christensen, J.H., Hewitson, B., Busuioc, A., Chen, A., Gao, X., Held, I., Jones, R., Kolli, R.K., Kwon, W.-T., Laprise, R., Magaña Rueda, V., Mearns, L., Menéndez, C. G., Räisänen, J., Rinke, A., Sarr, A., and Whetton, P.: Regional Climate Projections. In: Climate Change 2007: The Physical Science Basis. Contribution of Working Group I to the Fourth Assessment Report of the Intergovernmental Panel on Climate Change [Solomon, S., Qin, D., Manning, M., Chen, Z., Marquis, M., Averyt, K.B., Tignor, M., and Miller, H.L. (eds.)]. Cambridge University Press, Cambridge, United Kingdom and New York, NY, USA, 2007.

Comiso, J.C., Parkinson, C.L., Gersten, R., and Stock, L.: Accelerated decline in the Arctic sea ice cover. GEOPHYS RES LETT, 35, L01703, doi: 10.1029/2007GL031972, 2008.

Connolly, R., Connolly, M., Soon, W.: Re-calibration of Arctic sea ice extent datasets using Arctic surface air temperature records. HYDROLOG SCI J, 62, 1317–1340, doi: 0.1080/02626667.2017.1324974, 2017.

Costa, F.D., Acevedo, O.C., Mombach, J.C.M., Degrazia, G.A.: A simplified model for intermittent turbulence in the nocturnal boundary layer. J ATMOS SCI, 68, 1714–1729, doi: http://dx.doi.org/10.1175/2011JAS3655.1, 2011.

Coumou, D., Petoukhov, V., Rahmstorf, S., Petri, S., and Schellnhuber, H.J.: Quasi-resonant circulation regimes and hemispheric synchronization of extreme weather in boreal summer. P NATL ACAD SCI USA, 111, 12331–12336, doi: 10.1073/pnas.1412797111, 2014.

Cullather, R.I., and Bosilovich, M.G.: The moisture budget of the polar atmosphere in MERRA. J CLIMATE, 24, 2861–2879, doi: 10.1175/2010JCLI4090.1, 2011.

Cuzzone, J., and Vavrus, S.: The relationships between Arctic sea ice and cloud-related variables in the ERA-Interim reanalysis and CCSM3. ENVIRON RES Lett., 6, 014016, doi: 10.1088/1748-9326/6/1/014016, 2011.

Dee, D.P., Balmaseda, M., Balsamo, G., Engelen, R., Simmons, A.J., and Thépaut, J.-N.: Toward a consistent reanalysis of the climate system. B AM METEOROL SOC, 95, 1235–1248, doi: http://dx.doi.org/10.1175/BAMS-D-13-00043.1, 2014a.

Dee, D. P., Fasullo, J., Shea, D., Walsh, J. & National Centre for Atmospheric Research Staff (Eds): The climate data guide: atmospheric eanalysis: overview & comparison tables, retrieved from https://climatedataguide.ucar.edu/climate-data/atmospheric-reanalysis-overview-comparison-tables. Last modified 05 Nov 2014, 2014b.

Deser, C., and Teng, H.: Evolution of Arctic sea ice concentration trends and the role of atmospheric circulation forcing, 1979–2007. GEOPHYS RES LETT, 35, L02504, doi: 10.1029/2007GL032023, 2008.

Francis, J. A., and Vavrus, S. J.: Evidence linking Arctic amplification to extreme weather in mid-latitudes. GEOPHYS RES LETT, 39, 28 March, doi: 10.1029/2012GL051000, 2012.

Francis, J.A., Chan, W., Leathers, D.J., Miller, J.R., Veron, D.E.: Winter Northern Hemisphere weather patterns remember summer Arctic sea-ice extent. GEOPHYS RES LETT, 36, L07503, https://doi.org/10.1029/2009GL037274, 2009.

Francis, J. A., Vavrus, S. J. and Cohen, J.: Amplified Arctic warming and mid-latitude weather: new perspectives on emerging connections. WIRES CLIM CHANGE, 8, e474, doi: 10.1002/wcc.474, 2017.

Galperin, B., Sukoriansky, S. and Anderson, P. S.: On the critical Richardson number in stably stratified turbulence. ATMOS SCI LETT, 8, 65–69, doi: 10.1002/asl.153, 2007.

Gao, Y., Sun, J., Li, F., He, S., Sandven, S., Yan, Q., Zhang, Z., Lohmann, K., Keenlyside, N., Furevik, T., Suo, L.: Arctic sea ice and Eurasian climate: A review. ADV ATMOS SCI, 32, 92–114, https://doi.org/10.1007/s00376-014-0009-6, 2015.
Graversen, R.G., Maurtisen, T., Drijfhout, S., Tjernström, M., and Mårtensson, S.: Warm winds from the Pacific caused extensive Arctic sea-ice melt in summer 2007. CLIM DYNAM, 36, 2103–2112, doi: 10.1007/s00382-010-0809-z, 2011.
Handorf, D., Jaiser, R., Dethloff, K., Rinke, A., and Cohen, J.: Impacts of Arctic sea ice and continental snow cover changes on atmospheric winter teleconnections. GEOPHYS RES LETT, 42, 2367–2377. doi: 10.1002/2015GL063203, 2015.
Hassanzadeh, P., Kuang, Z., and B. F. Farrell: Responses of midlatitude blocks and wave amplitude to changes in the meridional temperature gradient in an idealized dry GCM. GEOPHYS RES LETT, 41, 5223–5232, doi: 10.1002/2014GL060764, 2014.
Herman, A. and Glowacki, O.: Variability of sea ice deformation rates in the Arctic and their relationship with basin-scale wind forcing. THE CRYOSPHERE, 6, 1553–1559, doi: 10.5194/tc-6-1553-2012, 2012.
Hutchings, J. K., Heil, P., and Hibler, W. D.: Modeling linear kinematic features in sea ice. MON WEATHER REV, 133, 3481–3497, doi: http://dx.doi.org/10.1175/MWR3045.1, 2005.
Inoue, J., Enomoto, T., Miyoshi, T., and Yamane, S.: Impact of observations from Arctic drifting buoys on the reanalysis of surface fields. GEOPHYS RES LETT, 36, L08501, doi: 10.1029/2009GL037380, 2009.
Inoue, J., Hori. M. E., Enomoto, T., Kikuchi T.: Intercomparison of surface heat transfer near the Arctic marginal ice zone for multiple reanalyses: A case study of September 2009. SOLA, 7, 057−060, doi: 10.2151/sola.2011-015, 2011.
IPCC, 2013: Climate Change 2013: The Physical Science Basis. Contribution of Working Group I to the Fifth Assessment Report of the Intergovernmental Panel on Climate Change [Stocker, T.F., D. Qin, G.-K. Plattner, M. Tignor, S.K. Allen, J. Boschung, A. Nauels, Y. Xia, V. Bex and P.M. Midgley (eds.)]. Cambridge University Press, Cambridge, United Kingdom and New York, NY, USA, 1535 pp, doi: 10.1017/CBO9781107415324, 2013.
Kahl, J.D.: Characteristics of the low-level temperature inversion along the Alaskan Arctic coast. INT J CLIMATOL, 10, 537–548, doi: 10.1002/joc.3370100509, 1990.
Koenigk, T., Caian, M., Nikulin, G., Schimanke, S.: Regional Arctic sea ice variations as predictor for winter climate conditions. CLIM DYNAM, 46, 317–337, doi: 10.1007/s00382-015-2586-1, 2016.
Lindsay, R., Wensnahan, M., Schweiger, A., and Zhang, J.: Evaluation of seven different atmospheric reanalysis products in the Arctic. J CLIMATE, 27, 2588–2606, doi: 10.1175/JCLI-D-13-00014.1, 2014.
Liu, Z., Schweiger, A., and Lindsay, R.: Observations and modeling of atmospheric profiles in the Arctic seasonal ice zone. MON WEATHER REV, 143, 39–53. doi: http://dx.doi.org/10.1175/MWR-D-14-00118.1, 2015.
Lüpkes, C., Vihma, T., Jakobson, E., König-Langlo, G., and Tetzlaff, A.: Meteorological observations from ship cruises during summer to the central Arctic: A comparison with reanalysis data. GEOPHYS RES LETT, 37, L09810, doi: 10.1029/2010GL042724, 2010.
Lüpkes, C., Gryanik, V.M., Rösel, A., Birnbaum, G. and Kaleschke, L.: Effect of sea ice morphology during Arctic summer on atmospheric drag coefficients used in climate models. GEOPHYS RES LETT, 40 , 1–6 . doi: 10.1002/grl.50081, 2013.

Mahrt, L.: Stably stratified boundary layer. In: Holton, J. P., Curry, J. A. and Pyle, J. (Eds.), Encyclopedia of Atmospheric Sciences. Academic Press, London, s. 298–305, 2002.

Mahrt L.: Stably stratified atmospheric boundary layers. ANN REV FLUID MECH, 46, 23–45, doi: 10.1146/annurev-fluid-010313-141354, 2014.

Maksimovich, E. and Vihma, T.: The effect of surface heat fluxes on interannual variability in the spring onset of snow melt in the central Arctic Ocean. J GEOPHYS RES, 117, C07012, doi: 10.1029/2011JC007220, 2012.

Mäkiranta, E., T. Vihma, A. Sjöblom, and Tastula, E.-M.: Observations and modelling of the atmospheric boundary layer over sea ice in a Svalbard fjord. BOUND-LAY METEOROL, 140, 105–123, doi: 10.1007/s10546-011-9609-1, 2011.

Navarro, J.C.A., Varma, V., Riipinen, I., Seland, O., Kirkevag, A. Struthers, H., Iversen, T., Hansson, H.C., Ekman, A.M.L.: Amplification of Arctic warming by past air pollution reductions in Europe. NAT GEOSCI, 9, 277–281, doi: 10.1038/ngeo2673, 2016.

Ogi, M., Yamazaki, Y., and Wallace, J. M.: Influence of winter and summer surface wind anomalies on summer Arctic sea ice extent. GEOPHYS RES LETT, 37, L07701, doi: 10.1029/2009GL042356, 2010.

Ogi, M. and Rigor, I.G.: Trends in Arctic sea ice and the role of atmospheric circulation. ATMOS SCI LETT, 14, 97–101, doi: 10.1002/asl2.423, 2013.

Onogi, K., Koide, M. Sakamoto, S. Kobayashi, J. Tsutsui, H. Hatsushika, T. Matsumoto, N. Yamazaki, H. Kanahori, K. Takahashi, K. Kato, R. Oyama, T. Ose, S. Kadokura and K. Wada: The JRA-25 reanalysis. J METEOROL SOC JPN, 85, 369–434, doi: 10.2151/jmsj.85.369, 2007.

Overland, J.E., Wang, M.: Large-scale atmospheric circulation changes associated with the recent loss of Arctic sea ice. TELLUS, 62, 1–9, https://doi.org/10.1111/j.1600-0870.2009.00421.x, 2010

Overland, J., Francis, J.A., Hall, R., Hanna, E., Kim, S.J., Vihma, T.: The melting Arctic and mid-latitude weather patterns: are they connected? J CLIMATE, 28, 7917–7932, doi: 10.1175/JCLI-D-14-00822.1, 2015.

Peings, Y. and Magnusdottir, G.: Response of the wintertime northern hemisphere atmospheric circulation to current and projected arctic sea ice decline: a numerical study with CAM5. J CLIMATE, 27, 244–264. doi: 10.1175/JCLI-D-13-00272.1, 2014.

Perlwitz, J., Hoerling, M., Dole, R.: Arctic tropospheric warming: causes and linkages to lower latitudes. J CLIMATE, 28, 2154–2167, doi: http://dx.doi.org/10.1175/JCLI-D-14-00095.1, 2015.

Petoukhov, V., and Semenov, V.A.: A link between reduced Barents-Kara sea ice and cold winter extremes over northern continents. J GEOPHYS RES-ATMOS, 115, D21111, doi: 10.1029/2009JD013568, 2010.

Petoukhov, V., Rahmstorf, S., Petri, S., and Schellnhube, H.J.: Quasiresonant amplification of planetary waves and recent Northern hemisphere weather extremes. P NATL ACAD SCI USA, 110, 5336–5341, doi: 10.1073/pnas.1222000110, 2013.

Proshutinsky, A. Y. and Johnson, M. A.: Two circulation regimes of the wind-driven Arctic Ocean. J. GEOPHYS RES, 102, 12493–12514, doi: 10.1029/97JC00738, 1997.

Proshutinsky, A., Steele, M., and Timmermans, M.-L.: Forum for Arctic Modeling and Observational Synthesis (FAMOS): Past, current, and future activities. J GEOPHYS RES-OCEANS, 121, 3803–3819, doi: 10.1002/2016JC011898, 2016.

Rampal, P., Weiss, J., Dubois, C., and Campin, J.-M.: IPCC climate models do not capture Arctic sea ice drift acceleration: Consequences in terms of projected sea ice thinning and decline. J GEOPHYS RES, 116, C00D07, doi:10.1029/2011JC007110, 2011.
Revelle, D.O. and Nilsson, E.D.: Summertime low-level jets over the high-latitude Arctic Ocean. J APPL METEOROL CLIM, 47, 1770–1784, doi: 10.1175/2007JAMC1637.1, 2008.
Rinke, A., Dethloff, K., Dorn, W., Handorf, D., and Moore, J.C.: Simulated Arctic atmospheric feedbacks associated with late summer sea ice anomalies. J GEOPHYS RES-ATMOS, 118, 7698–7714, doi: 10.1002/jgrd.50584, 2013.
Saha, S., Moorthi, S., Pan, H., Wu, X., Wang, J., Nadiga, S., et al.: The NCEP climate forecast system reanalysis. B AM METEOROL SOC, 91, 1015–1057. doi: 10.1175/2010BAMS3001.2.S1, 2010.
Sato, K., Inoue, J., and Watanab, M.: Influence of the Gulf Stream on the Barents Sea ice retreat and Eurasian coldness during early winter. ENVIRON RES LETT, 9, 084009, doi: 10.1088/1748-9326/9/8/084009, 2014.
Sato, K. and Inoue, J.: Comparison of Arctic sea ice thickness and snow depth estimates from CFSR with in situ observations. CLIM DYNAM, 50, 289–301, https://doi.org/10.1007/s00382-017-3607-z, 2018.
Screen, J.A., and Simmonds, I.: The central role of diminishing sea ice in recent Arctic temperature amplification. NATURE, 464, 1334–1337, doi: 10.1038/nature09051, 2010.
Screen, J.A. and Simmonds, I.: Erroneous Arctic temperature trends in the ERA-40 Reanalysis: A closer look. J CLIMATE, 24, 2620–2627, doi:10.1175/2010JCLI4054.1, 2011.
Screen, J.A., Deser, C., and Simmonds, I.: Local and remote controls on observed Arctic warming. GEOPHYS RES LETT, 39, L10709, doi: 10.1029/2012GL051598, 2012.
Screen, J.A., and Simmonds, I.: Exploring links between Arctic amplification and mid-latitude weather. GEOPHYS RES LETT, 40, 959–964, doi: 10.1002/grl.50174, 2013.
Screen, J.A. and Simmonds, I.: Amplified mid-latitude planetary waves favour particular regional weather extremes. NAT CLIM CHANGE, 4, 704–709, doi: 10.1038/nclimate2271, 2014.
Screen, J. A., Deser, C., Simmonds, I., and Tomas, R.: Atmospheric impacts of Arctic sea-ice loss, 1979–2009: Separating forced change from atmospheric internal variability. CLIM DYNAM, 43, 333–344, https://doi.org/10.1007/s00382-013-1830-9, 2014.
Serreze, M.C., and Francis, J.A.: The Arctic amplification debate. CLIMATIC CHANGE, 76, 241–264, doi: 10.1007/s10584-005-9017-y, 2006.
Serreze, M.C., Barrett, A.P., Stroeve, J.C., Kindig, D.N., and Holland, M.M.: The emergence of surface-based Arctic amplification. THE CRYOSPHERE, 3,11–19, doi: 10.5194/tc-3-11-2009, 2009.
Serreze, M.C. and Barry, R.G.: Processes and impacts of Arctic amplification: a research synthesis. GLOBAL PLANET CHANGE, 77, 85–96, doi: 10.1016/j.gloplacha.2011.03.004, 2011.
Serreze, M.C., Barrett, A.P., and Stroeve, J.: Recent changes in tropospheric water vapor over the Arctic as assessed from radiosondes and atmospheric reanalyses. J GEOPHYS RES, 117, D10104, doi10.1029/2011JD017421, 2012.

Simmonds, I.: Comparing and contrasting the behaviour of Arctic and Antarctic sea ice over the 35-year period 1979–2013. ANN GLASIOL, 56, 18–28, doi: 10.3189/2015AoG69A909, 2015.

Smedman, A.-S., Andre, U., Carlsson, M., Högström, U., Magnusson, M., Rost, J., and Zilitinkevich, S.: Surface-layer turbulence and the structure of the atmospheric boundary layer, in: BALTEX-BASIS Final Report, edited by: Launiainen, J. and Vihma, T., International BALTEX Secretariat, Publication, 19, 14–41, 2001.

Steeneveld, G.J., van de Wiel, B.J.H., and Holtslag, A.A.M.: Modelling the Arctic stable boundary layer and its coupling to the surface. BOUND-LAY METEOROL, 118, 357–378, doi: 10.1007/s10546-005-7771-z, 2006.

Stroeve, J., Holland, M.M., Meier, W., Scambos, T., and Serreze, M.: Arctic sea ice decline: Faster than forecast. GEOPHYS RES LETT, 34, L09501, doi: 10.1029/2007GL029703, 2007.

Stroeve, J. C., Serreze, M. C., Holland, M. M., Kay, J. E., Malanik, J., and Barrett, A. P.: The Arctic's rapidly shrinking sea ice cover: a research synthesis. CLIMATE CHANGE, 110, 1005–1027, doi: 10.1007/s10584-011-0101-1, 2012.

Stroeve, J. C., Markus, T., Boisvert, L., Miller, J., and Barrett, A.: Changes in Arctic melt season and implications for sea ice loss. GEOPHYS RES LETT, 41, 1216–1225, doi: 10.1002/2013GL058951, 2014.

Stull, R.: An introduction to boundary layer meteorology, Springer, 670 pages, 1988.

Stull, R.: Micrometeorology, Eos Trans. AGU, 90, 7, doi: 10.1029/2009EO010010, 2009.

Sun, L., Allured, D., Hoerling, M., Smith, L., Perlwitz, J., Murray, D., Eischeid, J.: Drivers of 2016 record Arctic warmth assessed using climate simulations subjected to Factual and Counterfactual forcing. WEATHER AND CLIMATE EXTREMES, 19, 1–9, https://doi.org/10.1016/j.wace.2017.11.001, 2018.

Suomi, I., Vihma, T., Gryning, S.-E., and Fortelius, C.: Wind gust parameterizations at heights relevant for wind energy – a study based on mast observations. Q J ROY METEOR SOC, 139, 1298–1310, doi: 10.1002/qj.2039, 2012.

Takhsha, M., Nikiéma, O., Lucas-Picher, P., Laprise, R., Hernández-Díaz, L., Winger K.: Dynamical downscaling with the fifth-generation Canadian regional climate model (CRCM5) over the CORDEX Arctic domain: effect of large-scale spectral nudging and of empirical correction of sea-surface temperature. CLIM DYNAM, 1–26, doi: 10.1007/s00382-017-3912-6, 2017.

Tang, Q., Zhang, X., Yang, X., and Francis, J.A.: Cold winter extremes in northern continents linked to Arctic sea ice loss. ENVIRON RES LETT, 8, 014036, doi: 10.1088/1748-9326/8/1/014036, 2013.

Thompson, D.W.J., and Wallace, J.M.: The Arctic Oscillation signature in the wintertime geopotential height and temperature fields. GEOPHYS RES LETT, 25, 1297–1300, doi: 10.1029/98GL00950, 1998.

Thorpe, A.J., and Guymer, T.H.: The nocturnal jet. Q J ROY METEOR SOC, 103, 633–653, https://doi.org/10.1002/qj.49710343809, 1977.

Tjernström, M., Leck, C., Persson, P.O.G., Jensen, M.L., Oncley, S.P., and Targino, A.: The summertime Arctic atmosphere: Meteorological measurements during the Arctic Ocean Experiment 2001. B AM METEOROL SOC, 85, 1305–1321, https://doi.org/10.1175/BAMS-85-9-1305, 2004.

Tjernström, M., Žagar, M., Svensson, G., Cassano, J., Pfeifer, S., Rinke, A., Wyser, K., Dethloff, K., Jones, C., Semmler, T., and Shaw, M.: Modelling the Arctic boundary layer: An evaluation of six Arcmip regional-scale models using data from the Sheba project. BOUND-LAY METEOROL, 117 (2), 337–381, doi: 10.1007/s10546-004-7954-z, 2005.

Tjernström, M., Birch, C. E., Brooks, I. M., Shupe, M. D., Persson, P. O. G., Sedlar, J., Mauritsen, T., Leck, C., Paatero, J., Szczodrak, M., and Wheeler, C. R.: Meteorological conditions in the central Arctic summer during the Arctic Summer Cloud Ocean Study (ASCOS). ATMOS CHEM PHYS, 12, 6863–6889, doi: 10.5194/acp-12-6863-2012, 2012.

Uotila, P., Vihma, T., and Haapala, J.: Atmospheric and oceanic conditions and the extremely mild Baltic Sea ice winter 2014/15. GEOPHYS RES LETT, 42, 7740–7749, doi: 10.1002/2015GL064901, 2015.

Vihma, T.: Effects of Arctic sea ice decline on weather and climate: A review. SURV GEOPHYS, 35, 1175–1214, doi: 10.1007/s10712-014-9284-0, 2014.

Vihma, T., Hartmann, J., and Lüpkes, C.: A case study of an on-ice air flow over the Arctic marginal sea-ice zone. BOUND-LAY METEOROL, 107, 189–217, https://doi.org/10.1023/A:1021599601948, 2003.

Vihma, T., and Pirazzini, R.: On the factors controlling the snow surface and 2-m air temperatures over the Arctic sea ice in winter. BOUND-LAY METEOROL, 117, 73–90, https://doi.org/10.1007/s10546-004-5938-7, 2005.

Vihma, T., Jaagus, J., Jakobson, E., and Palo, T.: Meteorological conditions in the Arctic Ocean in spring and summer 2007 as recorded on the drifting ice station Tara. GEOPHYS RES LETT, 35, L18706, doi:10.1029/2008GL034681, 2008.

Vihma, T., Kilpeläinen, T., Manninen, M., Sjöblom, A., Jakobson, E., Palo, T., Jaagus, J., and Maturilli, M.: Characteristics of temperature and humidity inversions and low-level jets over Svalbard fjords in spring. ADV METEOROL, 2011, 486807, doi:10.1155/2011/486807, 2011.

Walesby, K. T. and Beare, R. J.: Parametrizing the Antarctic stable boundary layer: synthesizing models and observations. Q J ROY METEOR SOC, 142, 2373–2385. doi: 10.1002/qj.2830, 2016.

Wallace, J.M., Mitchell, T.P., and Deser, C.: The influence of sea surface temperature on surface wind in the eastern equatorial Pacific: Seasonal and interannual variability. J CLIMATE, 2, 1492–1499, doi: 10.1175/1520-0442(1989)002<1492:TIOSST>2.0.CO;2, 1989.

Wallace, J.M., and Hobbs, P.V.: Atmospheric science – an introductory survey, 2nd edition, Academic Press, 483 p, 2006.

Walsh, J.E., and Chapman, W.L.: 20th-century sea-ice variations from observational data. ANN GLASIOL, 33, 444–448, doi: http://dx.doi.org/10.3189/172756401781818671, 2001.

Walsh, J.E.: Intensified warming of the Arctic: Causes and impacts on middle latitudes. GLOBAL PLANET CHANGE, 117, 52–63, https://doi.org/10.1016/j.gloplacha.2014.03.003, 2014.

Watanabe, E., and Ogi, M.: How does Arctic summer wind modulate sea ice-ocean heat balance in the Canada Basin? GEOPHYS RES LETT, 40, 1569–1574, doi: 10.1002/grl.50363, 2013.

Wilson, A.B., Bromwich, D.H., and Hines, K.M.: Evaluation of polar WRF forecasts on the Arctic system reanalysis domain: Surface and upper air analysis. J GEOPHYS RES, 116, D11112, doi: 10.1029/2010JD015013, 2011.

SUMMARY IN ESTONIAN

Tuulekiiruse, õhutemperatuuri ja merejää vastastikused mõjud Arktikas ning kaugseosed kliima varieeruvusega idapoolses Läänemere regioonis

Arktika kui uurimispiirkond on viimaste aastakümnetega oluliselt tähtsamaks muutunud. Peamiseks põhjuseks on Arktika regiooni kaks korda kiirem soojenemine ülejäänud kliimamuutuste taustal. Ennustatav püsijää kadumine Põhja-Jäämerelt juba võib-olla mõnekümne aasta pärast loob täiesti uued klimaatilised ja ökoloogilised olud lähis-arktilises vöötmes. Läbi kaugseoste (mis toimivad peamiselt üldise tsirkulatsiooni kaudu) mõjutavad muutused Arktikas ka teiste piirkondade ilma ja kliimat. Kahjuks on polaaralade geofüüsikaline uuritus olnud siiani puudulik. Meteoroloogilisi mõõtmisi on enamasti tehtud vaid rannikul ja saartel paiknevatest jaamadest. Kesk-Arktika piirkonnast on vaatlusandmeid väga vähe. Seetõttu on erinevus kliima prognooside osas väga suur ja ka järelanalüüsi mudelites on Arktika regioonis suured ebatäpsused.

Seoses neljanda rahvusvahelise polaaraastaga (2007–2008) toimus Euroopa Liidu programm DAMOCLES. Selle raames viidi läbi ulatuslikud mõõtmised Arktikas, et dokumenteerida merejää, atmosfääri ning ookeani muutusi. Triivjaam Tara oli üks vaatluste tegemise keskpunkt, mis triivis jääs Tiksist Teravmägedeni septembrist 2006 kuni jaanuarini 2008. Läbides Kesk-Arktika piirkonda 2007. aasta suvel (25. aprillist 31. augustini), viidi läbi ka atmosfääri meteoroloogilisi sondeerimisi. Tulemuseks oli 95 väga hea vertikaalse resolutsiooniga sondeerimist (andmed salvestati ca iga 5 meetri järel), mida ei kasutatud ühegi mudeli sisendina. See andis hea võimaluse kasutada sondeerimise andmeid järelanalüüsi mudelite valideerimisel. Andmete kõrge vertikaalne resolutsioon andis ka võimaluse uurida madalate jugavoolude olemasolu, omadusi ja tekkepõhjuseid.

Tara triivjaama andmed näitasid, et viie valideeritud mudeli (ERA-Interim, JCDAS, NCEP-CFSR, NCEP-DOE, NASA-MERRA) seast andis parimaid tulemusi ECMWF poolt loodud ERA-Interim. Siiski ei anna ükski mudel parimaid tulemusi kõikides muutujates ja kõikidel kõrgustel. ERA-Interimi tulemused olid parimad õhutemperatuuri süstemaatilise vea ja standardhälve osas, samuti tuulekiiruse süstemaatilise vea, standardhälve ning korrelatsiooni koefitsiendi osas. Samas pinnalähedaste parameetrite nagu 10 m tuule ja 2 m õhutemperatuuri osas andsid paremaid tulemusi NCEP-CFSR, NCEP-DOE, ja NASA-MERRA. Toetudes sellele teadmisele kasutati just NCEP-CFSR järelanalüüsi mudelit, et analüüsida pinnalähedaste tuulte ning merejää vahelisi seoseid.

Üks põhjustest, miks järelanalüüsi mudelites on Arktika piirkonnas suured vead, on madalate jugavoolude ebatäpne kirjeldamine stabiilse atmosfääri tingimustes. Kuigi madalaid jugavoole on vaatlusandmetega paremini varustatud aladel uuritud üpris palju, ei saa neid andmeid üle kanda Arktika keskosale, sest Arktika keskosas puuduvad nii tavapärane ööpäevane käik kui ka mägede mõju ja seetõttu ei saa madalate jugavoolude esinemissagedust, omadusi ning tekkemehhanisme üks-üheselt üle kanda lõunapoolsetelt vaatlustelt. Meile teada olevatel andmetel ei ole Arktika keskosas varasemalt läbiviidud ühtegi madalate jugavoolude uuringut. Meie analüüsi tulemustest selgus, et madalate jugavoolude esinemissagedus on väiksem nendest uuringutest, mis põhinevad Arktika ranniku ning saartel paiknevate jaamade andmetel. Kui saartel ja rannikul tehtud uuringute järgi on madalate jugavoolude esinemissagedus 60–80%, siis Tara triivjaama andmetel esineb madalaid jugavoole kõigest 46% sondeerimistest. Märkimisväärne erinevus võib tuleneda järgmistest asjaoludest: a) Taral läbiviidud sondeerimised toimusid kaugel barokliinsetest tsoonidest (jääpiirist, mägedest) b) suvisel poolaastal on atmosfääri stabiilsus väiksem kui talvisel poolaastal (mil enamus saartel ning rannikualade vaatlused oli tehtud). Erinevalt eelmistest lõunapoolsetest uuringutest joonistus välja keerulisem seos madalate jugavoolude tuuma kõrguse ning temperatuuri inversiooni tipu kõrguse vahel. Kui jugavoolu tuum asub turbulentses kihis, siis puudub korrelatsioon inversiooni tipuga; kui tuum asub turbulentsest kihist kõrgemal, siis on inversiooni tipuga tugev korrelatsioon (R = 0.72; $p < 0.01$). Vastupidiselt lõunapoolsete alade uuringutele esinesid barokliinse tekkepõhjusega jugavoolud madalamatel kõrgustel kui ülejäänud jugavoolud. See on tõenäoliselt seotud faktiga, et hõõrdumise poolt mõjutatud kiht on stabiilse stratifikatsiooni puhul õhuke. Kõige olulisem jugavoolude tekkepõhjus oli barokliinsus, mis tekitas tugevaid ja sooje keskmisest madalamaid jugavoolusid. Inertsiaalse ostsillatsiooni poolt põhjustatud madalad jugavoolud on tavaliselt seotud ööpäevase käiguga. Kesk-Arktikas ei saanud see olla põhjuseks. Inertsiaalse ostsillatsiooni poolt põhjustatud jugavoolud tekivad olukorras, kus atmosfääri stabiilsus taastub. Selline olukord võib tekkida näiteks pärast torme, samuti külmade frontide puhul, kui külm õhk tungib soojema õhu alla. Inertsiaalse ostsillatsiooni poolt põhjustatud madalate jugavoolude tuuma kiirus oli 1.5 ms^{-1} kõrgem ($p < 0.05$) kui ülejäänutel jugavooludel. Registreeritud jugavooludest 9% põhjustasid tuulepuhangud. Fronte ei defineeritud jugavoolude tekkemehhanismiks vaid jugavoolude soodustajaks, mil võivad koos esineda mitmed tekkemehhanismid. Põhjuseks on asjaolu, et mitte-okludeerunud frondid on barokliinsed, külmad frondid võivad soodustada inertsiaalset ostsillatsiooni ning tuuled on külmas õhumassis sageli puhangulised.

Jää negatiivne trend, mis on valdav olnud juba 20. sajandi keskpaigast, on viimasel kümnendil veelgi kiirenenud. Vaatlusperioodil 1979–2015 on tuvastatav 10 m tuule kiiruse positiivne trend, mis ulatub sügisel Tšukši meres 10%-ni keskmisest tuule kiirusest. Tulemused näitavad, et jää kontsentratsiooni ning 10 m tuule vahel valitseb tugev negatiivne seos nii sünoptilisel kui ka aastate vahelisel ajaskaalal. Seejuures on aastate vahelisel ajaskaalal korrelatsioon oluliselt tugevam. Kirjandusele toetudes on teada pinnalähedaste tuulte mõju jääle – läbi tugevamate pinnalähedaste tuulte suureneb lahvanduste pindala ning jäätriiv. Meie hüpotees oli, et on ka teistpidine seos. Seejuures keskendusime kõigepealt atmosfääri stabiilsuse muutusele seoses jää kontsentratsiooni muutusega. Kui jääd jääb vähemaks, siis üldreeglina pinnatemperatuur tõuseb ning atmosfääri stabiilsus väheneb. Erandiks on suvine atmosfäär Arktika keskosas.

Suvine atmosfäär võib jää vähenemise tõttu muutuda hoopis stabiilsemaks. Põhjuseks on asjaolu, et soolase vee külmumistemperatuur on allpool nulli (Põhja-Jäämeres ca –1,7 °C) ning sulamispiiril olev lumi, jää ning magedate sulavee lompide temperatuur on nulli lähedal. Atmosfääri stabiilsuse näitajana kasutasime oma analüüsis Richardsoni arvu, mis oli tugevas negatiivses korrelatsioonis 10 m tuultega. Seega vähem jääd tähendab väiksemat atmosfääri stabiilsust (välja arvatud suvel) ning see võimaldab suuremat impulsi ülekannet kõrgematest kihtidest madalamatesse ning põhjustab tugevamaid tuuli 10 m kõrgusel merepinnast. Teine viis kuidas jää kontsentratsioon saab mõjutab pinnalähedasi tuuli on pinnakihi karedus. Üldiselt on veepind siledam kui jääpind, aga see sõltub jää kontsentratsioonist ning ka lainetusest. Väiksema kui 70% jää kontsentratsiooni puhul üldiselt pinnakaredus jää vähenemisega väheneb. Kuna meid huvitavad kõige rohkem piirkonnad, kus trendid ja seosed on tugevaimad (st rannikumered), siis võime üldiselt öelda, et jää vähenemisega ka pinnakaredus väheneb. Kokkuvõtvalt, jää vähenemisega muutub atmosfäär ebastabiilsemaks ning pinnakaredus väiksemaks, seega 10 m tuuled tugevamaks. Järelikult on olemas vastastikune seos jää kontsentratsiooni ning pinnalähedaste tuulte vahel.

Suured muutused Arktikas ei mõjuta mitte üksnes Arktika kliima- ja ökosüsteemi, vaid ka piirkondi Arktikast väljaspool. Arktika seosed Põhja-Ameerika ja Aasia vahel on paremini läbi uuritud ning selgemad kui seosed Euroopaga. Meile teadaolevalt pole Läänemere ja Arktika vahelisi kaugseoseid siiamaani uuritud. Leidsime oma analüüsi tulemusena, et mitmete meteoroloogiliste parameetrite tugev kaugmõju Arktika ning Läänemere idapoolse regiooni vahel ei ole seletatav ainult kliimaindeksite abil. Näiteks on Arktika osade piirkondade jää kontsentratsioonil tugev kaugmõju Läänemere idapoolse piirkonna 1000 hPa temperatuuri ja tuulekiirusega kõikidel aastaaegadel. Külmade ja mahedamate talvede võrdlus näitas, et mahedamate talvede korral nihkub soe anomaalia mööda 60 laiuskraadi Gröönimaa kohalt ida poole ning jõuab Skandinaavia piirkonda järgmise aasta suveks. Füüsikalised seosed Arktika ning Läänemere idaosa piirkondade parameetrite kaugmõju kohta vajavad edasist uurimist.

ACKNOWLEDGEMENTS

Foremost I would like to thank my supervisors Prof. Jaak Jaagus and Dr. Erko Jakobson from the University of Tartu for continuous support, advice, cooperation and reviewing of the text of the papers. They lead me to the interesting Arctic meteorology and climatology topic. I thank the crew of Tara for their highly valuable contributions to the field work.

I am very grateful to Timo Vihma from Finnish Meteorological Institute for patience and guidance. He is one of the leading polar researchers and he really showed me the beauty of scientific thinking.

My gratitude goes to all co-authors for valuable scientific discussion and their contribution to data analysis and writing process.

I am sincerely grateful to my family for their strong support and understanding through the all doctoral time.

This research was supported by SA Archimedes project "Climate and environmental changes in polar regions related to global changes and their influence on climate variability in the northern Europe" (SLOOM12073T) and by the Estonian Research Council grant PUT (PUT645).

PUBLICATIONS

CURRICULUM VITAE

Name: Liisi Jakobson
Date of birth: 16. January 1980
Marital status: married, 3 children
Phone: +372 53 583 233
E-mail: liisi.jakobson@ut.ee

Education:

2010–…	PhD in Physical Geography, University of Tartu, theme 'Mutual effects of wind speed, air temperature and sea ice concentration in the Arctic and their teleconnections with climate variability in the eastern Baltic Sea region'.
2001–2005	BSc (equalized to MSc) (Cum Laude) in Physical Geography, University of Tartu.
1998–2005	BSc in Applied Computer Science, University of Tartu, Faculty of Mathematics and Computer Sciences.

Professional employment:

2015–…	Junior research fellow, Group of Remote Sensing of Atmosphere, University of Tartu, Faculty of Science and Technology, Tartu Observatory.
2013–2015	Specialist, Department of Geography, Institute of Ecology and Earth Science, University of Tartu.

Field of research

Physical geography, boundary layer meteorology in Polar Regions, the Arctic sea ice and interactions with near-surface winds, low-level jets, teleconnections.

Research Training:

August 2015	Doctoral Students Conference held by Baltic Earth, Estonia.
2014	ERCA (European Research Course on Atmospheres), Grenoble, France.

Publications

Jakobson, L., Jakobson, E., Post, P., Jaagus, J.: Atmospheric teleconnections between the Arctic and the eastern Baltic Sea regions. Earth System Dynamics, 8, 1019−1030, doi: 10.5194/esd-8-1019-2017, 2017.

Jakobson, L., Jakobson, E.: Atmospheric teleconnections between the Arctic and the eastern Baltic Sea regions. Poster presentation, American Geophysical Union (AGU), Fall General Assembly 2017, New Orleans, 11–15 December 2017.

Jakobson, L., Vihma, T., Jakobson, E.: How does the shrinking sea ice influence changing wind speed over the Arctic Ocean? Oral presentation, American

Geophysical Union (AGU), Fall General Assembly 2016, San Francisco, 12–16 December 2016.

Jakobson, L., Vihma, T., Jakobson, E., Palo, T., Männik, A., Jaagus, J.: Low-level jet characteristics over the Arctic Ocean in spring and summer. Atmospheric Chemistry and Physics, 13, 11089–11099, doi: 10.5194/acp-13-11089-2013, 2013.

Jakobson, E., Vihma, T., Palo, T., **Jakobson, L**., Keernik, H., Jaagus, J.: Validation of atmospheric reanalyses over the central Arctic Ocean. Geophysical Research Letters, 39, 1–6, doi: 10.1029/2012GL051591, 2012.

ELULOOKIRJELDUS

Nimi: Liisi Jakobson
Sünniaeg: 16.01.1980
Kodakondsus: Eesti
E-post: liisi.jakobson@ut.ee
Praegune töökoht, amet:
Tartu Ülikool, Loodus- ja täppisteaduste valdkond, Tartu Observatoorium, nooremteadur

Haridus

2010–...	Tartu Ülikool geograafia doktorantuur
2004–2005	Tartu Ülikool geograafia gümnaasiumi õpetaja
2001–2005	Tartu Ülikool geograafia
1998–2005	Tartu Ülikool rakendusinformaatika
1995–1998	Tartu Karlova Gümnaasium

Teenistuskäik

2015–…	Tartu Ülikool, Loodus- ja täppisteaduste valdkond, Tartu observatoorium, nooremteadur
2013–2015	Tartu Ülikool, Loodus- ja tehnoloogiateaduskond, Tartu Ülikooli Ökoloogia- ja Maateaduste Instituut, spetsialist

Peamised uurimisvaldkonnad

Füüsiline geograafia, piirkihi meteoroloogia polaaraladel, madalad jugavoolud, Arktika kaugmõju.

Publikatsioonid

Jakobson, L., Jakobson, E., Post, P., Jaagus, J.: Atmospheric teleconnections between the Arctic and the eastern Baltic Sea regions. Earth System Dynamics, 8, 1019−1030, doi: 10.5194/esd-8-1019-2017, 2017.

Jakobson, L., Vihma, T., Jakobson, E., Palo, T., Männik, A., Jaagus, J.: Low-level jet characteristics over the Arctic Ocean in spring and summer. Atmospheric Chemistry and Physics, 13, 11089–11099, doi: 10.5194/acp-13-11089-2013, 2013.

Jakobson, E., Vihma, T., Palo, T., **Jakobson, L.**, Keernik, H., Jaagus, J.: Validation of atmospheric reanalyses over the central Arctic Ocean. Geophysical Research Letters, 39, 1–6, doi: 10.1029/2012GL051591, 2012.

Konverentsiettekanded

Jakobson, L., Jakobson, E.: Atmospheric teleconnections between the Arctic and the eastern Baltic Sea regions. Posterettekanne. American Geophysical Union (AGU), Fall General Assembly 2017, New Orleans, USA, 11–15. detsember 2017.

Jakobson, L., Vihma, T., Jakobson, E.: How does the shrinking sea ice influence changing wind speed over the Arctic Ocean? Suuline ettekanne. American Geophysical Union (AGU), Fall General Assembly 2016, San Francisco, USA, 12–16. detsember 2016.

Jakobson, L., Jakobson, E.: Relationships between sea ice concentration and wind speed in the Arctic during 1979–2015. Posterettekanne. The Arctic Science Summit Week 2013, Krakow, Poola, 16–19. aprill 2013.

Projektid

PUT645 "Aerosoolide ja kasvuhoonegaaside panus kliima muutusesse Läänemere regioonis ja Arktikas", (01.01.2015–31.12.2018), Erko Jakobson, Tartu Ülikool.

SLOOM12073T "Polaaralade kliima- ja keskkonnamuutused seotuna globaalsete muutustega ning nende mõju Põhja-Euroopa kliima kõikumistele (1.01.2012−31.08.2015)", Jaak Jaagus, Tartu Ülikool.

Erialane enesetäiendus

2014 ERCA (European Research Course on Atmospheres) doktorikool, Grenoble, Prantsusmaa.

2015 Baltic Earth doktorantide konverents, Tartu, Eesti.

DISSERTATIONES GEOGRAPHICAE UNIVERSITATIS TARTUENSIS

1. **Вийви Руссак.** Солнечная радиация в Тыравере. Тарту, 1991.
2. **Urmas Peterson.** Studies on Reflectance Factor Dynamics of Forest Communities in Estonia. Tartu, 1993.
3. **Ülo Suursaar.** Soome lahe avaosa ja Eesti rannikumere vee kvaliteedi analüüs. Tartu, 1993.
4. **Kiira Aaviksoo.** Application of Markov Models in Investigation of Vegetation and Land Use Dynamics in Estonian Mire Landscapes. Tartu, 1993.
5. **Kjell Weppling.** On the assessment of feasible liming strategies for acid sulphate waters in Finland. Tartu, 1997.
6. **Hannes Palang.** Landscape changes in Estonia: the past and the future. Tartu, 1998.
7. **Eiki Berg.** Estonia's northeastern periphery in politics: socio-economic and ethnic dimensions. Tartu, 1999.
8. **Valdo Kuusemets.** Nitrogen and phosphorus transformation in riparian buffer zones of agricultural landscapes in Estonia. Tartu, 1999.
9. **Kalev Sepp.** The methodology and applications of agricultural landscape monitoring in Estonia. Tartu, 1999.
10. **Rein Ahas.** Spatial and temporal variability of phenological phases in Estonia. Tartu, 1999.
11. **Эрки Таммиксаар.** Географические аспекты творчества Карла Бэра в 1830–1840 гг. Тарту, 2000.
12. **Garri Raagmaa.** Regional identity and public leaders in regional economic development. Tartu, 2000.
13. **Tiit Tammaru.** Linnastumine ja linnade kasv Eestis nõukogude aastatel. Tartu, 2001.
14. **Tõnu Mauring.** Wastewater treatment weltlands in Estonia: efficiency and landscape analysis. Tartu, 2001.
15. **Ain Kull.** Impact of weather and climatic fluctuations on nutrient flows in rural catchments. Tartu, 2001.
16. **Robert Szava-Kovats.** Assessment of stream sediment contamination by median sum of weighted residuals regression. Tartu, 2001.
17. **Heno Sarv.** Indigenous Europeans east of Moscow. Population and Migration Patterns of the Largest Finno-Ugrian Peoples in Russia from the 18^{th} to the 20^{th} Centuries. Tartu, 2002.
18. **Mart Külvik.** Ecological networks in Estonia — concepts and applications. Tartu, 2002.
19. **Arvo Järvet.** Influence of hydrological factors and human impact on the ecological state of shallow Lake Võrtsjärv in Estonia. Tartu, 2004.
20. **Katrin Pajuste.** Deposition and transformation of air pollutants in coniferous forests. Tartu, 2004.

21. **Helen Sooväli.** *Saaremaa waltz*. Landscape imagery of Saaremaa Island in the 20th century. Tartu, 2004.
22. **Antti Roose.** Optimisation of environmental monitoring network by integrated modelling strategy with geographic information system — an Estonian case. Tartu, 2005.
23. **Anto Aasa.** Changes in phenological time series in Estonia and Central and Eastern Europe 1951–1998. Relationships with air temperature and atmospheric circulation. Tartu, 2005.
24. **Anneli Palo.** Relationships between landscape factors and vegetation site types: case study from Saare county, Estonia. Tartu, 2005.
25. **Mait Sepp.** Influence of atmospheric circulation on environmental variables in Estonia. Tartu, 2005.
26. **Helen Alumäe.** Landscape preferences of local people: considerations for landscape planning in rural areas of Estonia. Tartu, 2006.
27. **Aarne Luud.** Evaluation of moose habitats and forest reclamation in Estonian oil shale mining areas. Tartu, 2006.
28. **Taavi Pae.** Formation of cultural traits in Estonia resulting from historical administrative division. Tartu, 2006.
29. **Anneli Kährik.** Socio-spatial residential segregation in post-socialist cities: the case of Tallinn, Estonia. Tartu, 2006.
30. **Dago Antov.** Road user perception towards road safety in Estonia. Tartu, 2006.
31. **Üllas Ehrlich.** Ecological economics as a tool for resource based nature conservation management in Estonia. Tartu, 2007.
32. **Evelyn Uuemaa.** Indicatory value of landscape metrics for river water quality and landscape pattern. Tartu, 2007.
33. **Raivo Aunap.** The applicability of gis data in detecting and representing changes in landscape: three case studies in Estonia. Tartu, 2007.
34. **Kai Treier.** Trends of air pollutants in precipitation at Estonian monitoring stations. Tartu, 2008.
35. **Kadri Leetmaa.** Residential suburbanisation in the Tallinn metropolitan area. Tartu, 2008.
36. **Mare Remm.** Geographic aspects of enterobiasis in Estonia. Tartu, 2009.
37. **Alar Teemusk.** Temperature and water regime, and runoff water quality of planted roofs. Tartu, 2009.
38. **Kai Kimmel.** Ecosystem services of Estonian wetlands. Tartu, 2009.
39. **Merje Lesta.** Evaluation of regulation functions of rural landscapes for the optimal siting of treatment wetlands and mitigation of greenhouse gas emissions. Tartu, 2009.
40. **Siiri Silm.** The seasonality of social phenomena in Estonia: the location of the population, alcohol consumption and births. Tartu, 2009.
41. **Ene Indermitte.** Exposure to fluorides in drinking water and dental fluorosis risk among the population of Estonia. Tartu, 2010.

42. **Kaido Soosaar.** Greenhouse gas fluxes in rural landscapes of Estonia. Tartu, 2010.
43. **Jaan Pärn.** Landscape factors in material transport from rural catchments in Estonia. Tartu, 2010.
44. **Triin Saue.** Simulated potato crop yield as an indicator of climate variability in Estonia. Tartu, 2011.
45. **Katrin Rosenvald.** Factors affecting EcM roots and rhizosphere in silver birch stands. Tartu, 2011.
46. **Ülle Marksoo.** Long-term unemployment and its regional disparities in Estonia. Tartu, 2011, 163 p.
47. **Hando Hain.** The role of voluntary certification in promoting sustainable natural resource use in transitional economies. Tartu, 2012, 180 p.
48. **Jüri-Ott Salm.** Emission of greenhouse gases CO_2, CH_4, and N_2O from Estonian transitional fens and ombrotrophic bogs: the impact of different land-use practices. Tartu, 2012, 125 p.
49. **Valentina Sagris.** Land Parcel Identification System conceptual model: development of geoinfo community conceptual model. Tartu, 2013, 161 p.
50. **Kristina Sohar.** Oak dendrochronology and climatic signal in Finland and the Baltic States. Tartu, 2013, 129 p.
51. **Riho Marja.** The relationships between farmland birds, land use and landscape structure in Northern Europe. Tartu, 2013, 134 p.
52. **Olle Järv.** Mobile phone based data in human travel behaviour studies: New insights from a longitudinal perspective. Tartu, 2013, 168 p.
53. **Sven-Erik Enno.** Thunderstorm and lightning climatology in the Baltic countries and in northern Europe. Tartu, 2014, 142 p.
54. **Kaupo Mändla.** Southern cyclones in northern Europe and their influence on climate variability. Tartu, 2014, 142 p.
55. **Riina Vaht.** The impact of oil shale mine water on hydrological pathways and regime in northeast Estonia. Tartu, 2014, 111 p.
56. **Jaanus Veemaa.** Reconsidering geography and power: policy ensembles, spatial knowledge, and the quest for consistent imagination. Tartu, 2014, 163 p.
57. **Kristi Anniste.** East-West migration in Europe: The case of Estonia after regaining independence. Tartu, 2014, 151 p.
58. **Piret Pungas-Kohv.** Between maintaining and sustaining heritage in landscape: The examples of Estonian mires and village swings. Tartu, 2015, 210 p.
59. **Mart Reimann.** Formation and assessment of landscape recreational values. Tartu, 2015, 127 p.
60. **Järvi Järveoja.** Fluxes of the greenhouse gases CO_2, CH_4 and N_2O from abandoned peat extraction areas: Impact of bioenergy crop cultivation and peatland restoration. Tartu, 2015, 171 p.

61. **Raili Torga.** The effects of elevated humidity, extreme weather conditions and clear-cut on greenhouse gas emissions in fast growing deciduous forests. Tartu, 2016, 128 p.
62. **Mari Nuga.** Soviet-era summerhouses On homes and planning in post-socialist suburbia. Tartu, 2016, 179 p.
63. **Age Poom.** Spatial aspects of the environmental load of consumption and mobility. Tartu, 2017, 141 p.
64. **Merle Muru.** GIS-based palaeogeographical reconstructions of the Baltic Sea shores in Estonia and adjoining areas during the Stone Age. Tartu, 2017, 132 p.
65. **Ülle Napa**. Heavy metals in Estonian coniferous forests. Tartu, 2017, 129 p.